Graviational Waves from Feynman Diagrams

Lucien Huber

9/13/2022

Table of contents

Preface

This is a Quarto book. It is also hosted at github.io.

1 Introduction

The detection of gravitational waves by the Laser Interferometer Gravitational-Wave Observatory () and Virgo collaborations in 2016 [**LIGOScientific:2016aoc**] has sparked a new era of gravitational wave astronomy. The first detections were of Binary Black Hole () mergers. More recently, Binary Neutron Star () mergers [**LIGOScientific:2017vwq**] as well as Neutron Star ()-Black Hole () mergers have been detected [**LIGOScientific:2021qlt**]. Future detectors will further increase sensitivity and will be able to detect a wide range of astrophysical sources. Studying these gravitational waves signals gives us a very powerful new window into the universe. It allows us to study the properties of neutron stars and black holes, and the physics of compact object mergers, but also gives us a powerful testing apparatus for general relativity.

To detect these faint signals LIGO and Virgo, have been made to be extraordinarily precise instruments. Thus, they demand correspondingly precise theoretical predictions and models. This is not just for comparison's sake, but for detection as well. These faint signals are often buried in the noise of the detector. To counteract this experimental physicists make use of a matched filtering approach, where they try to match the signal to a template. The template is a model of the signal ideally provided by theoretical physicists based on physical theories. The more precise the template, the higher the signal-to-noise ratio, the more probable and precise the detection.

In this thesis we will explore the theoretical landscape surrounding the generation of these templates. We will focus on a nascent subfield where tools originally used for Quantum Field Theory () and particle physics are being applied to the study of gravitational waves. Specifically we are interested

in the diagrammatic objects that arise when framing the two body problem similarly to particle collisions. We will explain where these tools shine in the broader context of waveform approaches such as Effective One-Body (), Nonrelativistic General Relativity (), Post-Minkowski () and Post-Newtonian () approximations. The document is organized as follows. The first section we deal with the theoretical foundations of gravitational waves, exploring how they come about if one linearizes Einsteins' field equations. The subsequent section discusses the experimental apparatuses that are used to detect gravitational waves. We look at the techniques used to extract the signals for the noise, and look at the motivation for precise theoretical predictions. In section 3 we look at how to generate partial and full waveforms. We explore the EOB and Numerical Relativity () frameworks. Motivated by the need for more precise ingredients to input into EOB, in Section 4 we look at the state of the art formalsims that incorporate amplitudes tools into the program. We take a look at the conservative Effective Field Theory () matching approach as well as the fully dissipation including Kosower Maybee and O'Connell () formalism. This is where we take a deeper look at the amplitude computing tools, and how they apply in this specific application. We close with a discussion of the challenges that lie ahead, and the future of gravitational wave astronomy.

2 Gravitational Wave Generation

First let us look at where and how gravitional waves are generated. We will look at how General Relativity () predicts that graviational waves exist, and what conditions have to be met for them to become observable. We will also look at how we can detect them, and what we can learn from them.

2.1 Gravitational Waves

The most complete theory of gravity we have right now is that of GR, due to Einstein. It formulates spacetime as a Riemannian manifold with curvature, senstive to mass. Objects then move around in that deformed spacetime encoded in the metric $g_{\mu\nu}$. Objects interact gravitationally when the spacetime they move around in is affected by the curvature caused by other objects. The equation that governs this interaction between mass and curvature is Einstein's field equations,

$$\boxed{R_{\mu\nu} - \frac{g_{\mu\nu}}{2}R + \Lambda g_{\mu\nu} = -8\pi G T_{\mu\nu}}. \qquad (2.1)$$

The Left-Hand Side () of this equation, contains several objects that are all only really dependent on the metric $g_{\mu\nu}$. $R_{\mu\nu}$ is the Ricci tensor[1], a contraction of the Riemann curvature tensor $R^{\beta}{}_{\mu\nu\rho}$. This tensor[2] encodes the curvature of spacetime, as it is essentially a measurement of the amount with which covariant derivatives don't commute. When they do, it means that they have collapsed to regular derivatives, and thus the Levi-civita connection[3] must have vanished. This is only possible if the metric is flat $\eta_{\mu\nu}$. The Riemann curvature tensor is exclusively made up of the metric, its first, second derivatives and it is linear in the second derivative of the metric. In fact it is the only possible tensor of that sort.

---

[1] The Ricci Tensor is given by:

$$R_{\mu\nu} := R^{\alpha}{}_{\mu\alpha\nu} = g^{\alpha\beta}R^{\alpha\mu\beta\nu}$$

[2] The Riemann Tensor is given by:

$$R^{\beta}{}_{\mu\nu\rho} = \Gamma^{\beta}{}_{\mu\nu,\rho} - \Gamma^{\beta}{}_{\mu\rho,\nu} - \Gamma^{\alpha}{}_{\mu\rho}\Gamma^{\beta}{}_{\alpha\nu} + \Gamma^{\alpha}{}_{\mu\nu}\Gamma^{\beta}{}_{\alpha\rho}.$$

[3] The Levi-Civita Connection is given by:

$$\Gamma^{\alpha}{}_{\mu\nu} = \frac{1}{2}g^{\alpha\rho}\left\{g_{\rho\nu,\mu} + g_{\rho\mu,\nu} - g_{\mu\nu,\rho}\right\}$$

The second term on the LHS is the Ricci scalar, a further contraction of the Ricci Tensor: $R = g^{\mu\nu} R_{\mu\nu}$. The final term on the LHS is just a proportional constant factor of the metric, where Λ is called the cosmological constant. It can be measured and has a low known upper bound. It is in part responsible for the expansion of the universe.

The Right-Hand Side () of 2.1 encodes the effect of mass and energy on the metric. $T_{\mu\nu}$ is the stress-energy tensor, dependent on the dynamics of the system. In empty space this term is zero. It is further multiplied by the Gravitational constant G.

Equation 2.1 can be recast in a form where the Ricci scalar has been eliminated,

$$R_{\mu\nu} = -8\pi G \left(T_{\mu\nu} - T^\alpha_{\ \alpha} \frac{g_{\mu\nu}}{2} \right) + \Lambda g_{\mu\nu} \qquad (2.2)$$

Either equation 2.1, 2.2 with $\Lambda = 0$ admit wave solutions. We can see this by looking at these equations in the weak field approximation. Namely, we take the metric to be a Minkowskian background and a small perturbation

$$g_{\mu\nu} = \eta_{\mu\nu} + h_{\mu\nu}, \qquad (2.3)$$

with $h_{\mu\nu}$ small. Note that if we restrict ourselves to first order in $h_{\mu\nu}$ then all raising and lowering of indices has to be done with $\eta_{\mu\nu}$, or else we increase the order of the term by 1. Now since the LHS of 2.1 is made up of the Ricci tensor and scalar, let us see how these behave in the weak approximation. Both are in fact made up of Levi-Civita connections, which to first order in $h_{\mu\nu}$ is given by:

$$\Gamma^\alpha_{\ \mu\nu} = \frac{1}{2} \eta^{\alpha\rho} \left\{ h_{\rho\nu,\mu} + h_{\rho\mu,\nu} - h_{\mu\nu,\rho} \right\} + \mathcal{O}(h^2) \quad . \qquad (2.4)$$

Plugging in to the definition of the Ricci tensor we see that the terms with products of the connection vanish, and we are left with the derivative terms:

$$R_{\mu\nu} = \frac{\eta^{\alpha\rho}}{2} \left[h_{\rho\alpha,\mu\nu} + h_{\mu\nu,\rho\alpha} - h_{\mu\alpha,\rho\nu} - h_{\nu\rho,\mu\alpha} \right] + \mathcal{O}(h^2) = R^{(1)}_{\ \mu\nu} + \mathcal{O}(h^2)$$
$$(2.5)$$

The linearized Ricci scalar is then just $R^{(1)} = \eta^{\mu\nu}R^{(1)}{}_{\mu\nu}$. Regardless of the weak approximation, 2.1 has some gauge freedom. This means that if we solve eq 2.1, it won't be the only possible solution, and in fact we can generate the others by changing coordinated in such a way that the equation isn't effected. To fix this ambiguity we choose a coordinate system ('gauge'), by imposing the harmonic coordinate conditions:

$$g^{\alpha\beta}\Gamma^{\mu}{}_{\alpha\beta} = 0 \qquad (2.6)$$

The harmonic coordinate conditions demand the vanishing of the Levi-Civita connection. They have a simplified form in the weak approximation, which we can acces by plugging 2.4 into 2.6, giving:

$$(\eta^{\alpha\beta} + h^{\alpha\beta})\frac{1}{2}(\eta^{\mu\rho} + h^{\mu\rho})\left[h_{\alpha\rho,\beta} + h_{\beta\rho,\alpha} - h_{\alpha\beta,\rho}\right] = 0$$
$$\eta^{\mu\rho}\eta^{\alpha\beta}\left[2h_{\alpha\rho,\beta} - h_{\alpha\beta,\rho}\right] + \mathcal{O}(h^2) = 0$$
$$\eta^{\alpha\beta}h_{\alpha\rho,\beta} = \frac{1}{2}h_{\alpha\beta,\rho}\eta^{\alpha\beta} + \mathcal{O}(h^2).$$

The last equation to first order is called the de Donder gauge and is often written:

$$h_{\mu\nu}{}^{,\mu} = \frac{1}{2}h^{\alpha}{}_{\alpha,\nu}$$

In de Donder gauge we can simplify the terms in 2.5 to:

$$\eta^{\alpha\beta}h_{\alpha\mu,\nu\beta} \approx \frac{1}{2}\eta^{\alpha\beta}h_{\alpha\beta,\mu\nu},$$

and

$$\eta^{\alpha\beta}h_{\beta\nu,\mu\alpha} \approx \frac{1}{2}h_{\alpha\beta,\mu\nu}.$$

With these two relations the expression for the linearized Ricci tensor 2.5 simplifies to

$$R^{(1)}{}_{\mu\nu} = \frac{1}{2}\eta^{\alpha\beta}h_{\mu\nu,\alpha\beta} = \frac{1}{2}\Box_{SR}h_{\mu\nu}. \qquad (2.7)$$

Where we have defined the Special Relativity () D'Alembertian as: $\Box_{SR} = \eta^{\mu\nu}\partial_{\mu}\partial_{\nu}$ We can plug this into 2.2, with $\Lambda = 0$, and up to first order in $h_{\mu\nu}$ we get the linearized Einstein field equations for a system of harmonic coordinates:

$$\square_{SR}h_{\mu\nu} = -16\pi G \overbrace{(T_{\mu\nu} - \frac{\eta_{\mu\nu}}{2}T^\alpha_{\ \alpha})}^{S_{\mu\nu}} \qquad (2.8)$$

$$h^\alpha_{\ \mu,\alpha} = \frac{1}{2}h^\alpha_{\ \alpha,\mu}. \qquad (2.9)$$

Where raising and lowering indices has been done with the Minkowski metric. The tensor $S_{\mu\nu}$ encodes the behavior of the source of gravitional waves. One could also plug 2.7 into 2.1, with $\Lambda = 0$, and if we change to the trace reversed perturbation: $\bar{h}_{\mu\nu} = h_{\mu\nu} - \frac{1}{2}h^\alpha_{\ \alpha}\eta_{\mu\nu}$, we get similar and simpler equations at the cost of a more complex perturbation: [4] [5]

$$\square_{SR}\bar{h}_{\mu\nu} = -16\pi G T_{\mu\nu} \qquad (2.10)$$

$$\bar{h}_{\mu\nu}{}^{,\nu} = 0. \qquad (2.11)$$

In this form we can very easily recover the conservation equation for the stress-energy tensor. We take the divergence of 2.10 and use 2.11 to get:

$$T_{\mu\nu}{}^{,\nu} = 0. \qquad (2.12)$$

Let us look at what sorts of solutions come out of these equations.

2.2 Homogenous solutions

The simplest first step is to consider the homogeous solution, as all solutions will involve these terms. Setting $T_{\mu\nu} = 0$ or $S_{\mu\nu} = 0$ yields an easily recognisable wave equation.

$$\square_{SR}h_{\mu\nu} = 0 \qquad (2.13)$$

The de Donder gauge (2.9) and the remaining gauge freedom[6] restricts the possible forms of this solution to having only helicity ± 2 physically significant components (see **Weinberg:1972**). Let us look at its generic form. The metric $h_{\mu\nu}$ ought to be real-valued, thus we seek real solutions of the form

[4] Note that the inverse change of variables is just: $h_{\mu\nu} = \bar{h}_{\mu\nu} - \frac{1}{2}\bar{h}^\alpha_{\ \alpha}\eta_{\mu\nu}$.

[5] We eliminate the trace of the stress-energy tensor by using: $R = 8\pi G T^\alpha_{\ \alpha}$. We can write $R^{(1)} = -\frac{1}{2}\square_{SR}\bar{h}^\alpha_{\ \alpha}$, in de Donder gauge, which is precisely the extra term dropping out of $\square_{SR}h_{\mu\nu}$ when we express it in terms of $\bar{h}_{\mu\nu}$

[6] from changes in coordinates such as $x^\mu \to x^\mu + \xi^\mu$ with $\square_{SR}\xi^\mu = 0$

$$h_{\mu\nu} = \varepsilon_{\mu\nu}\mathrm{e}^{i k \cdot x} + \varepsilon^*{}_{\mu\nu}\mathrm{e}^{-i k \cdot x},$$

where $\varepsilon_{\mu\nu}$ is the polarization tensor and k is the wave vector. The polarization tensor is a symmetric rank-2 tensor, since $h_{\mu\nu}$ is. Additionally we define:

$$k \cdot x \equiv \eta_{\mu\nu}k^{\mu}k^{\nu} = k_{\mu}x^{\mu}.$$

Substituting into $\square_{SR}h_{\mu\nu} = 0$ gives $k_{\mu}k^{\mu} \equiv k^2 = 0$[7] [8]. From 2.9 we have

$$\varepsilon^{\mu}{}_{\nu}k_{\mu} = \frac{1}{2}\varepsilon^{\alpha}{}_{\alpha}k_{\nu}. \tag{2.14}$$

As said at the beginning of this subsection, we still have some remaining gauge freedom, which we now fix, choosing the following coordinate change $x^{\mu} \to x^{\mu} + \zeta^{\mu}$ where:

$$\zeta^{\mu} = i A^{\mu}\mathrm{e}^{i k \cdot x} = -i A^{*\mu}\mathrm{e}^{-i k \cdot x}$$

Imposing this change yields the following modified perturbation:

$$h'_{\mu\nu} = h_{\mu\nu} - \frac{\partial \zeta_{\mu}}{\partial x^{\nu}} - \frac{\partial \zeta_{\nu}}{\partial x^{\mu}} = \varepsilon'_{\mu\nu}\mathrm{e}^{i k \cdot x} + \varepsilon'^{*}{}_{\mu\nu}\mathrm{e}^{-i k \cdot x}.$$

with

$$\varepsilon'_{\mu\nu} = \varepsilon_{\mu\nu} + k_{\mu}A_{\nu} + k_{\nu}A_{\mu} \tag{2.15}$$

Equations 2.14 and 2.15 reduce the free components in the polarization tensor to just two. Additionally these equations can conspire to yield a traceless polarisation tensor $\varepsilon^{\alpha}{}_{\alpha} = 0$, with $\varepsilon_{0\mu} = 0$ (see **Carroll:2019**). This then extends to the metric perturbation, which when imposed to be traceless, becomes equal to its trace-reversed counterpart. This is the so-called transverse traceless gauge:

$$h_{0\mu} = 0, \quad h^{\alpha}{}_{\alpha} = 0, \quad h_{\mu\nu}{}^{,\nu} = 0.$$

The metric perturbation in this gauge is written as: $h^{TT}{}_{ij}$.

[7] assuming non-zero perturbation $h_{\mu\nu}$ of course

[8] this is saying that the wavevector for the wave is null, thus that the wave propagates at the speed of light

2.3 Inhomogenous solutions

With the homogenous part of 2.8 accounted for, we can now look at the inhomogenous part. The solution in the presence of a source term of 2.8 will be heavily inspired by the analogous problem in electromagnetism. If we define the following retarded Green's function

$$\mathcal{G}_{\text{ret}}(x^\mu - x'^\mu) = -2\pi\,\delta^4((x^\mu - x'^\mu)^2)\Theta(x^0 > x'^0),$$

which satisfies,

$$\Box_{SR}\mathcal{G}_{\text{ret}}(x^\mu - x'^\mu) = \delta^4(x^\mu - x'^\mu).$$

Then, the solution to

$$\Box_{SR}h_{\mu\nu} = -16\pi G S_{\mu\nu} \qquad (2.16)$$

is given by:

$$h_{\mu\nu}(x) = 8G \int \mathrm{d}^4x' \; \mathcal{G}_{\text{ret}}(x^\mu - x'^\mu)S_{\mu\nu}(x'), \qquad (2.17)$$

since when we plug in 2.17 into 2.16

$$\Box_x h_{\mu\nu} = 8G \int \mathrm{d}^4x' \; ((\underbrace{\Box_x \mathcal{G}_{\text{ret}}(x^\mu - x'^\mu)}_{=-2\pi\,\delta(x^\mu - x'^\mu)})S_{\mu\nu}(x') = -16\pi G S_{\mu\nu}(x)$$

One gets the parallel solution to the trace reversed equation 2.10 by swapping S with T and all h with $\bar{h}$

We can perform the $x'^0 = t'$ integration in 2.17, with the delta function, setting $t' = t - |x^\mu - x'^\mu| = t_r$ the retarded time, i.e:

$$h_{\mu\nu}(x) = 8G \int \mathrm{d}^3\mathbf{y}\, S_{\mu\nu}(t, \mathbf{y})\, \mathrm{d}t'\, \frac{\delta(t' - (t - |\mathbf{x} - \mathbf{y}|))}{2|\mathbf{x} - \mathbf{y}|}$$

$$h_{\mu\nu}(\mathbf{x}, t) = 4G \int \mathrm{d}^3\mathbf{y}\, \frac{S_{\mu\nu}(t - |\mathbf{x} - \mathbf{y}|, \mathbf{y})}{|\mathbf{x} - \mathbf{y}|}. \qquad (2.18)$$

We can interpret the solution at $(\mathbf{x}, t)$ above, as the perturbation due to the sumed up contributions of all the sources at the point $(\mathbf{x} - \mathbf{y}, t_r)$ on the past light cone. Put differently this will be the gravitational radiation produced by the source $S_{\mu\nu}$.

Additionally, the form of the time argument of the source tensor, imposed by the definition of the Green's function, shows that the radiation propagates with velocity $= 1 = c$. This retarded solution satisfies the harmonic coordinate condition of 2.8, as required. Indeed, we have

$$T_{\mu\nu;\mu} = 0 \;\Rightarrow\; T_{\mu\nu,\mu} + \underbrace{\Gamma\,\Gamma}_{\text{non−linear}} = 0 \;\Rightarrow\; T_{\mu\nu,\mu} = 0,$$

ignoring non-linearities. Then,

$$S^{\mu\nu}{}_{,\mu} = \partial_\mu \left(T_{\mu\nu} - \frac{\eta^{\mu\nu}}{2} T^\alpha{}_\alpha \right) = -\frac{\eta^{\mu\nu}}{2} T^\alpha{}_{\alpha,\mu}.$$

Also

$$S^\mu{}_\mu = T^\mu{}_\mu - \frac{\delta^\mu_\mu}{2} T^\alpha{}_\alpha = -T^\alpha{}_\alpha.$$

Thus

$$S^{\mu\nu}{}_{,\mu} = \frac{1}{2} S^\alpha{}_{\alpha,\mu} \eta^{\mu\nu}$$
$$S^\mu{}_{\nu,\mu} = \frac{1}{2} S^\alpha{}_{\alpha,\nu}.$$

Then

$$h^{\mu}{}_{\nu,\mu} = 8G \frac{\partial}{\partial x^{\mu}} \int \mathrm{d}^4 x' \, \mathcal{G}_{\mathrm{ret}}(x^{\mu} - x'^{\mu}) S^{\mu}{}_{\nu}(x')$$

$$= 8G \int \mathrm{d}^4 x' \, \frac{\partial \mathcal{G}_{\mathrm{ret}}(x^{\mu} - x'^{\mu})}{\partial x^{\mu}} S^{\mu}{}_{\nu}(x')$$

$$= -8G \int \mathrm{d}^4 x' \, \frac{\partial \mathcal{G}_{\mathrm{ret}}(x^{\mu} - x'^{\mu})}{\partial x'^{\mu}} S^{\mu}{}_{\nu}(x')$$

$$= \underbrace{8G \mathcal{G}_{\mathrm{ret}}(x^{\mu} - x'^{\mu}) \delta^{\mu}_{\nu}(x')}_{=0 \text{ for } x=x'} + 8G \int \mathrm{d}^4 x' \, \mathcal{G}_{\mathrm{ret}}(x^{\mu} - x'^{\mu}) \frac{\partial S^{\mu}{}_{\nu}(x')}{\partial x'^{\mu}}$$

$$= 8G \int \mathrm{d}^4 x' \, \mathcal{G}_{\mathrm{ret}}(x^{\mu} - x'^{\mu}) \frac{1}{2} \frac{\partial S^{\alpha}{}_{\alpha}(x')}{\partial x'^{\mu}}$$

$$= \quad \dots \quad \text{repeat in reverse}$$

$$= \frac{\partial}{\partial x^{\mu}} \left\{ 8G \int \mathrm{d}^4 x' \, \mathcal{G}_{\mathrm{ret}}(x^{\mu} - x'^{\mu}) \frac{1}{2} S^{\alpha}{}_{\alpha}(x') \right\}$$

$$= \frac{1}{2} h^{\alpha}{}_{\alpha,\mu}. \checkmark$$

2.4 Gravitational Wave Sources

Now that we have the general form of the solutions to the linearized Einstein equations, we can proceed to the analysis of the sources of gravitational waves. The first step is to analyse the equations in the frequency domain. We will use the following notation:

$$\mathcal{F}_t [\phi] (\omega, \mathbf{x}) = \int \mathrm{d}t \, \phi(t, \mathbf{x}) \mathrm{e}^{i \omega t}$$

$$\mathcal{F}_{\omega}^{-1} [\phi] (t, \mathbf{x}) = \int \frac{\mathrm{d}\omega}{2\pi} \mathcal{F}_t [\phi] (\omega, \mathbf{x}) \mathrm{e}^{-i \omega t}$$

Let us look at the trace reversed solution, as the conservation

equation for

$$\mathcal{F}_t\left[h_{\mu\nu}\right](\omega, \mathbf{x}) = \int \mathrm{d}t\, h_{\mu\nu}(t, \mathbf{x})\mathrm{e}^{i\omega t}$$

$$= 4G \int \mathrm{d}^3\mathbf{y}\,\mathrm{d}t\, \frac{S_{\mu\nu}(t - |\mathbf{x} - \mathbf{y}|, \mathbf{y})}{|\mathbf{x} - \mathbf{y}|}\mathrm{e}^{i\omega t}$$

$$= 4G \int \mathrm{d}^3\mathbf{y}\,\mathrm{d}t_r\, \frac{S_{\mu\nu}(t_r, \mathbf{y})}{|\mathbf{x} - \mathbf{y}|}\mathrm{e}^{i\omega t_r}\mathrm{e}^{i\omega|\mathbf{x} - \mathbf{y}|}$$

$$= 4G \int \mathrm{d}^3\mathbf{y}\, \frac{\mathcal{F}_{t_r}\left[S_{\mu\nu}\right](\omega, \mathbf{y})}{|\mathbf{x} - \mathbf{y}|}\mathrm{e}^{i\omega|\mathbf{x} - \mathbf{y}|}$$

$$(2.19)$$

We can now apply various approximations to this form of the perturbation. The first is to consider that we look at the radiation only in the so called *wave zone*, at a distance $r = |\mathbf{x}|$ much larger than the dimensions of the source $R = |\mathbf{y}|_{\text{max}}$. Additionally we assume that $r \gg \frac{1}{\omega}$, i.e long wavelengths don't dominate. Finally we assume that $r \gg \omega R^2$, i.e. the ratio of R to the wavelength is not comparable to the ratio of r to R. Using this approximation we can write:

$$|\mathbf{x} - \mathbf{y}| = r\left(1 - 2\hat{\mathbf{x}} \cdot \mathbf{y} + \frac{\mathbf{x}'^2}{r^2}\right)^{1/2}$$

$$|\mathbf{x} - \mathbf{y}| \approx r\left(1 - \frac{\hat{\mathbf{x}} \cdot \mathbf{y}}{r}\right) \quad \text{with: } \hat{\mathbf{x}} = \frac{\mathbf{x}}{r}.$$

If we additionally further separate the scales in the following way[9]

$$r \gg [\frac{1}{\omega}, \omega R^2] \gg R,$$

Then 2.19 becomes much simpler[10]:

$$\mathcal{F}_t\left[h_{\mu\nu}\right](\omega, \mathbf{x}) = 4G\frac{\mathrm{e}^{i\omega r}}{r}\int \mathrm{d}^3\mathbf{y}\, \mathcal{F}_t\left[S_{\mu\nu}\right](\omega, \mathbf{y}) \quad (2.20)$$

Now let us look at the fourier transform of the source term. By definition we have

[9] we just add the condition that $\frac{1}{\omega} \gg R$, that is the source radius is much smaller than the wavelength

[10] the approximations all conspire to be able to neglect the $\mathbf{y}$ dependence of $\mathrm{e}^{i\omega|\mathbf{x} - \mathbf{y}|}$ in the integral

$$\mathscr{F}_t\left[S_{\mu\nu}\right](\omega,\mathbf{y}) = \mathscr{F}_t\left[T_{\mu\nu}\right](\omega,\mathbf{y}) + \tfrac{1}{2}\eta_{\mu\nu}\mathscr{F}_t\left[T^{\alpha}{}_{\alpha}\right](\omega,\mathbf{y})$$

Thus the term to analyse is actually $\mathscr{F}_t\left[T_{\mu\nu}\right]$. We can use the conservation equation 2.12 in fourrier t-space to write:

$$-\mathscr{F}_t\left[T_{i\mu}\right]^{,i} = \mathring{\imath}\omega\mathscr{F}_t\left[T_{0\mu}\right] \qquad (2.21)$$

This equation becomes algebraic when we further fourrier transorm in $\mathbf{x}$-space:

$$\hat{T}_{\mu\nu}(k^{\alpha}) = \hat{T}_{\mu\nu}(\omega,\mathbf{k}) = \int \mathrm{d}^3\mathbf{y}\,\mathscr{F}_t\left[T_{\mu\nu}\right](\omega,\mathbf{y})\mathrm{e}^{\mathring{\imath}\mathbf{k}\cdot\mathbf{y}}$$

Then the conservation equation becomes:

$$k^{\mu}T_{\mu\nu}(\omega,\mathbf{k}) = 0$$

These four equations enable us to just care about the purely spacelike components of $T_{\mu\nu}$. Let us apply 2.21 to itself to obtain:

$$\mathscr{F}_t\left[T_{ij}\right]^{,ij} = -\omega^2\mathscr{F}_t\left[T_{00}\right]$$

which when multiplied by $x_m x_n$ and integrated over $\mathbf{x}$ gives[11]:

$$\int \mathrm{d}\mathbf{x}\,\mathscr{F}_t\left[T_{mn}\right](\omega,\mathbf{x}) = -\frac{\omega}{2}\int \mathrm{d}\mathbf{x}\,x_m x_n\mathscr{F}_t\left[T_{00}\right](\omega,\mathbf{x})$$

Notice the last integral is in fact the fourrier transform of (a third of) the quadrupole moment tensor of the energy denisty:

$$I_{mn} = \int x_m x_n T_{00}(t,\mathbf{x})\,\mathrm{d}^3x\,. \qquad (2.22)$$

We call its fourrier transform $\hat{I}_{mn}(\omega)$ and we can finally rewrite 2.20 as:

$$\mathscr{F}_t\left[h_{\mu\nu}\right](\omega,\mathbf{x}) = -2G\omega^2\frac{\mathrm{e}^{\mathring{\imath}\omega r}}{r}(\hat{I}_{mn}(\omega) + \tfrac{1}{2}\eta_{\mu\nu}\hat{I}^n{}_n(\omega))$$

---

[11] two integrations by parts cancels the $x_m x_n$ term in the LHS, since boundary terms are 0 (the source is finite) we have

$$\int \mathrm{d}x\,x_m x_n\mathscr{F}_t\left[T_{ij}\right]^{,ij} = \int \mathrm{d}x\,x_m x_n{}^{,ij}\mathscr{F}_t\left[T_{ij}\right]$$

The hessian of $x_m x_n$ is $(\delta^i_m + \delta^i_n)(\delta^j_n + \delta^j_m)$, but since $T_{\mu\nu}$ is symmetric the integral is

$$\int \mathrm{d}\mathbf{y}\,2\mathscr{F}_t\left[T_{mn}\right](\omega,\mathbf{y})$$

Going back t-space we have:

$$
\begin{aligned}
h_{\mu\nu}(t,\mathbf{x}) &= -\frac{G}{\pi r}\int \mathrm{d}\omega\, \mathrm{e}^{-i\omega(t-r)}\omega^2(\hat{I}v_{mn}(\omega) + \tfrac{1}{2}\eta_{\mu\nu}\hat{I}^n{}_n(\omega)) \\
&= \frac{G}{\pi r}\frac{\mathrm{d}^2}{\mathrm{d}t^2}\int \mathrm{d}\omega\, \mathrm{e}^{-i\omega(t_r)}(\hat{I}_{mn}(\omega) + \tfrac{1}{2}\eta_{\mu\nu}\hat{I}^n{}_n(\omega)) \\
&= \frac{2G}{r}\frac{\mathrm{d}^2}{\mathrm{d}t^2}(I_{mn}(t_r) + \tfrac{1}{2}\eta_{\mu\nu}I^n{}_n(t_r))
\end{aligned}
$$
(2.23)

This equation has a very nice physical interpretation. The gravitational wave produced by a non-relativistic source is proportional to the second derivative of the quadrupole moment of the its energy denisty at the time where the past light cone of the observer intersects the source (t_r). The nature of gravitational radiation is in stark contrast to the leading electromagnetic contribution which is due the the change in the *dipole* moment of the charge density. The change of the dipole moment can be attributed to the change in center of charge (for Electromagnetism ()), or mass (for GR), and while a center of charge is free to move around, the center of mass (of an isolated) is fixed by the conservation of momentum. The quadrupole moment, on the other hand, is sensitive to the shape of the source, which a gravitional system can modify. Finally the quadrupole radiation is subleading when compared to dipole radiation. Thus on top of the much smaller coupling constant, gravitional radiation is also weakened by this fact, and thus is usually orders of magnitude weaker than electromagnetic radiation.

Thus any object that is modifying its shape is a source of gravitational waves. All orbiting systems therefore are sources of Gravitational Wave ()s. However as said just above, only very important 'changes in shape' have a chance to be detectable. These phenomena are what we will explore next.

2.4.1 Compact binaries

How could one construct a very powerful source of GWs? One could take two very massive objects, (such that T_{00} is large) and make them orbit each other. At that point one could hope to detect this orbit if the objects are massive enough and orbiting close enough for the 'change in shape' of the system

to sizeable. For these very massive objects to be close enough for a small orbit, they have to be very compact. Assuming that is the case, a funny thing happens, as these objects orbit each other, they emit GWs, and in doing so they lose energy[12]. Thus they slow down, and their orbit shrinks. This continues until the orbit is so small that the objects merge into a single object. Of course this is a very important change of shape and thus we have a constructed (if not all on purpose) a very powerful source of GWs. Such objects are called compact binaries.

To Leading Order () we can use a newtonian circular orbit to describe the motion of the binary. nsuch a system is in fact equivalent to effective one body [13] of reduced mass $\mu = \frac{m_1 m_2}{M}$ orbiting in a gravitional potential of mass $M = m_1 + m_2$, at a distance R equal to the distance between the binary. Such an orbit can easily be characterized by a balancing act between the gravitational attraction due to the potential and the centripetal force due to the motion of the reduced mass:[14]

$$\frac{GM\mu}{(R)^2} = \frac{\mu u^2}{R},\qquad(2.24)$$

where u is the norm of tangential velocity, and R is the distance between the two objects. 2.24 gives us the the norm of the velocity:

$$u = \sqrt{\frac{GM}{R}}.$$

Thus the orbital period is simply, in the case of

$$T = \frac{2\pi R}{u} = 2\pi\sqrt{\frac{R^3}{GM}}.$$

This also gives us angular frequency:

$$\Omega = \frac{2\pi}{T} = \sqrt{\frac{GM}{R^3}}.\qquad(2.25)$$

Thus the Equation of Motion () $\mathbf{r}(t)$ of the reduced mass is, in a circular orbit, in the $x - y$ plane:

[12] of course this happens in every orbiting system just on a time scale that is neglible. Only systems which are massive enough to produce large amounts of radiation actually lose enough energy for it to matter

[13] This choice of wording is nota coincidence as we shall see

[14] or equivalently between conserved angular momentum and the derivative of the potential energy

$$\mathbf{r}_{xy}(t) = \begin{pmatrix} R\cos(\Omega t) \\ R\sin(\Omega t) \end{pmatrix}.$$

The corresponding EOM for both masses is simply given by applying the following scaling:

$$\mu\mathbf{r}(t) = m_1\mathbf{r}_2(t) = m_2\mathbf{r}_2(t).$$

We can straightforwardly obtain the 00 component of the energy momentum tensor of the system[15] by using the EOM of the reduced mass:

[15] the energy density is the same for the effective one body system and the two body system

$$T_{00}(t,\mathbf{x}) = \mu\delta(x_3)\delta(x_1 - R\cos(\Omega t))\delta(x_2 - R\sin(\Omega t)).$$

Which when plugged into 2.22 gives us the quadrupole moment of the the rotating system:

$$I_{11} = \mu R^2\cos^2(\Omega t) = \mu R^2(1 + \cos(2\Omega t))$$
$$I_{22} = \mu R^2\sin^2(\Omega t) = \mu R^2(1 - \cos(2\Omega t))$$
$$I_{12} = I_{21} = 2\mu R^2(\cos\Omega t)(\sin\Omega t) = \mu R^2\sin(2\Omega t)$$
$$I_{i3} = 0.$$

Thus we have roughly:

$$I \sim \mu R^2\cos(2\Omega t) \sim \mu R^2 \sim \mu\left(\frac{GM}{\Omega^2}\right)^{\frac{2}{3}} = \frac{Gm_1m_2}{(m_1 + m_2)^{\frac{1}{3}}}\Omega^{-\frac{4}{3}},$$

where we have expanded in small R in the second relation. The metric perturbation is then given by 2.23 and has norm ignoring constants:

$$h \sim \frac{\ddot{I}}{r} \sim \frac{1}{r}\frac{Gm_1m_2}{(m_1 + m_2)^{\frac{1}{3}}}\Omega^{\frac{2}{3}}. \tag{2.26}$$

2.4.2 BH Binaries

Taking the process described above to the limit one could imagine asking for the most dense objects possible to orbit each other. In GR this object is called a black hole (BH). It is a possible solution to the full fat Einstein Field Equations () (2.1), where we consider a static and isotropic universe, with point like mass at its center. Then the solutions to the equations 2.1 have a unique form [**Birkhoff:1923**], called the Schwarzschild solution. The solution is given by, in spherical coordinates:

$$\mathrm{d}\tau^2 = \left[1 - \frac{R_S}{r}\right]\mathrm{d}t^2 - \frac{\mathrm{d}r^2}{1 - \frac{R_S}{r}} - r^2\left(\mathrm{d}\theta^2 + \sin^2\theta\,\mathrm{d}\varphi^2\right)$$

(2.27)

where R_S is the Schwarzschild radius, given by:[16]

$$R_S = \frac{2GM}{c^2}.$$

For stellar masses we have $R_S = 2954$ m, quite a lot smaller than the radius of the sun $\sim 7\cdot10^8$ m. Note that 2.27 exhibits singularities (blowing up of the metric compontents) at both $r = R_S$ and $r = 0$. The former is spurious, as it is an artefact of the coordinate choice, while the latter is real, in the sense that coordiante independent scalars formed from the metric (such as the ricci scalar) do in fact blow up as $r \to 0$. This encodes the very real mass singularity of what we call a BH.

If we consider a compable stellar mass binary black hole system, we can use the calculations of the previous section to compute the order of magnitude of the perturbation. 2.25 in terms of the Schwarzschild radius gives us the orbital frequency:

$$f = \frac{\Omega}{2\pi} \approx \frac{c}{2\pi}\sqrt{\frac{R_S}{R^3}}$$

and the metric perturbation is given by 2.26:

$$h \approx \frac{R_S^2}{rR}.$$

[16] we reinstate the speed of light, as we want to compute orders of magnitudes

Now if we consider BHs separated by ten times their Schwarzschild radius, at cosmological distances ~ 100 Mpc, we have the following scales:

$$R_S \approx 10^3 \text{ m}$$
$$R \approx 10^4 \text{ m}$$
$$r \approx 10^{23} \text{ m}.$$

Such a system would have an orbital frequency of:

$$f \approx 10^2 \text{ Hz},$$

and would perturb the metric on earth by:

$$h \approx 10^{-21}.$$

To have any hope of detecting such systems, one would need to have detectors sensitive in the hundreds of Hertz, with a strain sensitivity of 10^{-21}. This has been achieved at LIGO and other detectors, and has enabled the detection of such systems.

2.4.3 NS Binaries

We can also not go as far as having our compact object be a BH, but can also consider NSs. These object are notheless extremely dense (not infinitely so), and are essentially like big atomic nuclei. Not much is known about them and in fact GW astronomy is could be

2.4.4 Exotic Sources

Cosmic strings, supernovae, and other exotic sources of GWs are also possible.

3 Gravitational Wave Detection

Gravitational waves were first theorized by Einstein, accompanying his theory of general relativity. However, it was not even clear whether this was an artifact of the theory or something real. Of course as we have seen, GWs are predicted to be very weak, and thus there initially very little hope of ever detecting them. As evidence mounted that GR was indeed a very good theory of gravity, people started to investigate more seriously whether one could detect GWs. The first detectors were resonant antennas, however, these have to date, not been successful in detecting GWs. The more modern laser based detectors were the final piece of the puzzle. With extremely high precision (the modern measurement accuracy at LIGO is equivalent to measuring the distance to Alpha Centauri to the width of a human hair), these detectors are able to detect GWs. The first detection was made in 2015, marking the beginning of a new era in astronomy, and maybe even physics itself.

3.1 Laser interferometers

Laser-interferometer based GW detectors are essentially scaled up versions of the Michelson interferometer. This device splits a beam of colimated coherent photons (laser) into two, letting them propagate along two axes in an L configuration, before being reflected back to the beam splitter. The two beams when recombined, interfere with each other, constructively or destructively, dependent on the nature of the medium they have traveled through and the length of each arm.

For a gravitiational wave to have an effect on such an apparatus, all the otpical equipment should be free to move and be isolated from external vibrations as much as possible. This is achieved by handing the mirror on precisely tuned

pendulums. When the gravitational wave propagates through the apparatus, it will effectively induce a relative movement between the masses, changing the difference $L_x - L_y$ in length of the detectors arms, by an amount ΔL. This effect will be exaserbated as the length of the arms $L_x \sim L_y \sim L$ is increased and thus we must normalise by it to get the strain h:

$$\frac{\Delta L}{L} = \left[(1/2)\left(1 + \cos^2(\theta)\right)\cos(2\phi)\right]h_+ + [\cos(\theta)\sin(2\phi)]h_\times \equiv h$$

where θ and ϕ are the polar and azimuthal angles of the direction of propagation of the GW. The strain is decomposed into components, h_+ and $h_\times$, which are the plus and cross polarisations of the wave. The strain sensitivity can be further increased by bouncing the light back and forth multiple times along the arms of the interferometer. In current implementations this is achieved using fabry - perot cavities spanning the whole length of the arms.

3.1.1 LIGO and ground based observatories

LIGO implements the measurement apparatus described in the past section. In consists of two detectors, both in the USA, one in Livingston Louisiana and one in Hanford Washington, a separation of 3000 km. Each LIGO detector has two 4 km long arms made up of 1.2 m-wide vacuum tubes, each operating as fabry-perot cavities. The light from an effective 750 kW laser bounces back and forth inside these arms around 300 times. Thus the effective arm length becomes 1200 km, drastically improving sensitivity.

LIGO while it was in fact the first to provide detection data, it does not live in a vacuum. In fact for the first published detection, the data analysis teams from LIGO joined forces with those for Virgo, the european gravitational wave detector forming a collaboration. The Virgo detector is located in Cascina, Italy, and is very similar to LIGO. It has 3 km long arms and a different suspension system. It joined data collection with LIGO in the second observing run in 2017. Finally there are two other detectors that are now part of the collaboration, KAGRA in Japan and GEO600 in Germany.

KAGRA is a similar detector to Virgo in scale, but is built underground further isolating it from seismic activity and GEO600 is a smaller detector, with 600 m long arms, built more as a test bed for future detectors.

These ground base detectors, although already exhibiting impressive sensitivity, are still limited by the fact that they are on the ground. This means that they are subject to seismic activity, which can cause vibrations that limits the lower bound of the frequency sensitivity of the detectors. The optics and other higher frequency noise imposes an upper bound to the frequency. Thus ground based detectors are only sensitive to frequencies in the following rough range:

$$[10^0, 10^4] \text{ Hz}.$$

This means that they are sensitive to the comparable, stellar mass [17] compact binaries, what we think to be the most common type of binary in the universe. Of course this is not an accident, as these detectors were purpose built for providing evidence of GW in general. In fact they have been quite successful in this regard, with the now upwards of 90 detections of GW to date.
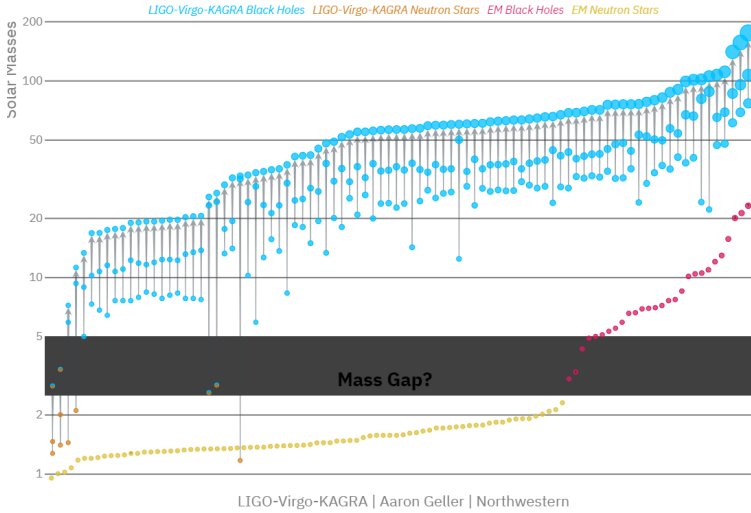
[17] and a bit bigger $\sim 1 - 10^3 M_\odot$

Fig 3.1: Mass distribution of Detected GW emiting binaries. Credit: Visualization: LIGO-Virgo-KAGRA / Aaron Geller / Northwestern

In Figure 3.1, the current library of compact binary systems detected by LIGO-Virg-Kagra is shown along with those detected through non GW means. The highlighted band

denotes the assumed mass gap that should exist between the neutron star and black hole mass distributions. Note that most of the detections are compatible with the presence of such a gap. However ,there are a few that are not, and these are the ones that are most interesting. These are binaries with masses too light to be black holes, but too heavy to be neutron stars, and a lot of research is ongoing to try and understand what these objects are, and if they are not just measurement artefacts.

3.1.2 Laser Interferometer Space Antenna ()

TODO

3.2 Matched filtering

The signals measured by the laser interferometers such as LIGO, are a measurement of strain over time. This waveform essentially measures the deformation of spacetime when a GW passes through a detector. While some GW signals coming out of laser interferometers, are clearly identified as such, mainly due to their extraordinary power output, smaller systems and weaker signals are harder to identify. In fact most of the detections have happened under the noise floor of the detectors. How is this possible? Matched filtering and waveform generation. In this section we will explain the matched filtering approach.

Consider some detector output signal s consisting of noise n and a possible true GW signal h_i (or signals, making up a family $\{h_i\}$). The nature of the noise is unpredictable and necessarily probabilistic in nature. We can however, model the noise as a random variable n with some probability distribution P_n, dependent on variables that we consider and have measured to be significantly impactful.

In such a probabilistic setup one could try to find the probability that the signal $h_i \in \{h_i\}$ has been detected, conditional on the actual data s. This however is impractical as it requires *a priori* knowledge on the family of possible signals, information totally inaccessible to us. Instead, we can devise a functional $\mathcal{F}[s, h_i]$, (statistic) dependent on both the data

and the supposedly present GW signal. We can then choose a threshold ρ^* above which we claim detection of the signal h_i, i.e. if $\mathcal{F}[s, h_i] > \rho^*$.

The functional that is used is based on the symmetric inner product $\langle s, h_i \rangle$, that correlates the data s with the template h_i, weighting by detector frequency sensitivity:

$$\langle g, h \rangle = 2 \int_{-\infty}^{\infty} \frac{\hat{g}^*(f)\hat{h}(f)}{S_n(|f|)} \, \mathrm{d}f = 4\Re \int_0^{\infty} \frac{\hat{g}^*(f)\hat{h}(f)}{S_n(f)} \, \mathrm{d}f,$$

where $\hat{g}^*$ is the conjugate of the frequency Fourier transform of g. $S_n(f)$ is the *noise power spectral density*, characterising the detector sensitivity defined by:

$$\overline{\hat{n}^*(f_1)\hat{n}(f_2)} = \tfrac{1}{2}\delta(f_1 - f_2)S_n(f_1)\Theta(f_1),$$

where the bar denotes the average over the noise realisation, $\delta(f_1 - f_2)$ is the Dirac delta function, and $\Theta(f_1)$ is the Heaviside step function. We can now define the *signal to noise ratio* for the signal when filtered by h_i as [18]

$$\rho(h_i) = \frac{\langle s, h_i \rangle}{\mathrm{rms}\langle n, h_i \rangle} = \frac{\langle s, h_i \rangle}{\sqrt{\langle h_i, h_i \rangle}}.$$

where rms denotes the root mean square. This is the functional $\mathcal{F}[s, h_i]$ we are after and we claim detection if $\rho(h_i) > \rho^*$. If the noise is normally distributed it can in fact be proven to be the optimal filtering technique, in the sense that it minimises the probability of false positives. For example, if we have a fully gaussian noisy signal $s = n$ then ρ is a normal variable centered on zero with unit variance. If there is some signal h_i present, over some still gaussian noise n then it can be proven that ρ is still normal but centered on $\sqrt{\langle h_i, h_i \rangle}$ with unit variance.

The threshold can be set ty correspond to a desired false positive rate:[19]

$$\mathcal{F} = \sqrt{\frac{1}{2\pi}} \int_{\rho^*}^{\infty} \mathrm{e}^{-\frac{1}{2}\rho^2} \, \mathrm{d}\rho = \tfrac{1}{2} \mathrm{erfc}(\frac{\rho^*}{\sqrt{2}}),$$

[18] The equality is due to the fact that we average over all realisations of noise, which averrages to uniform: $\overline{\langle h_i, n \rangle \langle n, h_i \rangle} = \langle h_i, h_i \rangle$

[19] The complementary error function is given by $\mathrm{erfc}(z) = \frac{2}{\sqrt{\pi}} \int_z^{\infty} \mathrm{e}^{-t^2} \, \mathrm{d}t = 1 - \mathrm{erf}(z)$.

26

or correct detection rate:

$$\mathcal{D} = \frac{1}{2}\operatorname{erfc}\left[\frac{\rho^* - \sqrt{\langle h_i, h_i\rangle}}{\sqrt{2}}\right].$$

Now given a signal and a template we have a procedure to determine if the signal is present or not. The physics output of a detection is therefor upper bounded by the physics content of the template. The matched filtering approach is contingent on having a waveform that corresponds to the physical process that is emitting the signal. Usually these processes can be parametrized by a set of parameters, such as in the case of a compact binary, the mass ratio of the binary, the orbit eccentricity, the possible spin etc. The filter waveform must then of course depend on these parameters, be it heuristically or physically (i.e., from first principles).

3.3 Pulsar Timing Array ()

A PTA consists of an array of several pulsars whose pulse periods (or Time of Arrival ()) are monitored with very high precision by one or more radio telescopes. Pulsars, from **pulsa**ting **r**adio source, are though to be highly magnetized rotating neutron stars. These neutron stars emit string electromagnetic radiation from their magnetic poles, which when not aligned with rotational poles, emit in the manner of a lighthouse. The measured pulses are extremely regular in nature, with periods ranging from a few milliseconds to a few seconds. Over a year the variation in the pulse period is on the order of a few microseconds [**Detweiler:1979wn**]. We can therefor use these as clocks, and measure their variation from their normal cycle time.

If a gravitational wave is between the pulsar and the observer, then the radio wave emitted by the pulsar will be effectively by travelling in a medium with anisotropic refractive index. This will cause the pulse to be delayed, or sped up, depending on the relative direction of the wave, it's polarization axes and the direction of the pulsar. If one has a collection of such pulsars with precisely known periods, evenly distributed in the celestial sphere, then one can use the relative delay of the pulses to measure the direction and nature of the wave.

nthe setup is essentially a blown up version of LIGO with light-year scale arms instead of kilometer scale arms.

Currently the set of pulsars suitable for this type of measurement is around 40 [**Maiorano:2021**]. Many more pulsars have been measured but not all are suitably regular to be used in PTAs. The frequency range of sensititivity of PTAs has a lowe bound set by observation duration and higher bound set by cadence of measurement. Currently the IPTA **Hobbs:2009yy** has been measuring for 13 years, with measurements being taken every week yielding a sensitivity in a drastically different band than that of LIGO and LISA:

$$[10^{-9}, 10^{-7}]\text{Hz}.$$

The nature of sources that can be detected by PTAs is therefor different from that of LIGO and LISA. The PTA sensitivity is more suited to detect stochastic gravitational waves, such as those emitted by the early universe, or by the supermassive black holes $(10^6 - 10^9 M_\odot)$ in the centers of galaxies[20].

[20] more massive objects have longer orbital periods

4 Waveform Generation

The matched filtering approach introduced in the previous section motivates tools for generating waveforms. Specifically the matched filtering technique is especially sensitive to the phase of the GW, necessitating very precise waveforms in the phase. These can be varied in physical content, but also in practicality. In all cases they need to be able to cover the set of parameters (the parameter space) that one is interested in exploring. Clearly if the waveform has been generated purely heuristically, then the physical content of the detection is close to zero. One can only say one has detected a phenomenon that produces this waveform, but not much more. However, if the input parameters are physically meaningful, like the mass ratio of a binary compact inspiraling system, then the waveform constructed purely from this input, if matched to the signal, tells us that a compact binary inspiraling system with this mass ratio has been detected. This is called parameter estimation, and is key to maximsing the physics output of a detection.

Crucially the waveform generation must be able to cover the whole parameter space (for example all feasible mass ratios) to be useful, as one does *not* know the parameters of the object one is looking for. Ideally this waveform generation can be done in a way that is computationally efficient, as the number of parameters to explore can be large. In the end, currently, waveform generation is done in a hybrid way, where some waveforms at some parameter space points are generated from first principles, and the rest of the parameter space waveforms are interpolated.

In this chapter we will look at the physically motivated waveform generation tools currently being developed in research. More specifically we are going to explore techniques for compact binary waveforms. Of these, there are two types, the inspiralling binaries, and the scattering ones. Currently only the inspiralling binaries have been detected, as these are the

systems for which LIGO and others are most sensitive to (see Section 3.1.1) and they are by far the most common emitters of high intensity GWs. As discussed in Section 2.4.1, orbiting and GW emitting compact objects will necessarily inspiral and merge at somepoint.

For such inspiraling binaries, the waveform has three distinct parts, corresponding to distinct phases of a binary merger: a first inspiral phase, a merger phase where a remnant compact body is produced as a result of the coalescence of the two objects, and a postmerger, or ringdown phase where the remnant still emits gravitational radiation while settling to its new stable configuration. Each phase has specific characteristics in the dynamics of the objects and thus correspondingly different frameworks are aimed at specific portions of the waveforms. Even within one phase, different regimes and thus frameworks exist, additionally dependent to the type/initial state of the two orbiting bodies.

For scattering binaries there is hope of detecting them **Mukherjee:2020hnm**, but they are mainly used as a testbed for new theories making use of particle physics knowledge. Additionally one might be able to extend their validity to inspiraling binaries [**Kalin:2019rwq**].

Most of these techniques have two important parts. The first consists in the precise modelling of the evolution of the emitting system. In most cases, this boils down to obtaining the EOMs for the interacting bodies, however for scattering this can just be the amplitude of the event. The second part is extracting the variation of the metric due to the source movement at the measurement point, far away from the source, i.e., the waveform. Of course the metric at the source is tightly coupled to the dynamics of the system, and thus the approximations conducted at the source also effects the way one extracts the waveform.

The only full, physically motivated waveform techniques are NR and EOB[21]. NR is quite unique when compared to other methods. Let us look at it now before proceeding to EOB and all the partial waveform techniques.

[21] There are a whole family of phenomenological frameworks that we will not discuss

30

4.1 NR

The most precise physically motivated waveform-generation technique to date is numerical relativity (NR). It was first developed as early as the 1960s [**hahn:1964**]. Initially and until relatively recently, these numerical methods were unusable because of numerical instabilities. The idea, however, is simple: the EFE are a system of coupled partial differential equations (PDEs) (albeit quite nonlinear) that can be solved numerically by discretizing the fields involved, i.e. the metric in this case. The cause of instability, and the difficult nature of the problem is three-fold. First, the aforementioned non-linearities make the discretization particularly sensitive, and means that one needs a fine mesh to control error buildup. Second, the gauge freedom that simplified the derivation in the last chapter, puts limits on the type of discretization procedure, so that spurious modes are not introduced. Third, for BHs one needs to consider what to do about the physical metric singularity, as infinity is not a number one can plug into a computer! On top of stability problems, when compact binary objects are considered, the scales involved further complicate things, as one needs enough resolution to resolve the objects, and the deformations on the metric, as well as a large enough volume to have reasonable orbits. This leads to a huge amount of points in the model, meaning such simulations (even if stable) are extremely computationally expensive.

In 2005 **Pretorius:2005gq** and a little later **Campanelli:2005dd** made a breakthrough advance and were able to fully compute an inspiral-merger-ringdown sequence for a BBH. Pretorius made use of two techniques, Adaptive Mesh Refinement () and the Generalized Harmonic () formalism. AMR, like its name suggests dynamically modified the discretiztation as the two black holes orbited each other. The GH formalism, on the other hand tackled the singularity problem validating the excision of the black hole, and crucially letting that region move. Both combined, were able to finally slay the proverbial numerical dragon.

These waveforms, like the one in Figure 4.1 confirmed the predictions made in **Buonanno:2000ef**, that the merger phase of a BBH would not be as complicated as thought. As numercal techniques evolved further, they were able to elucidate more and more complex behaviors.
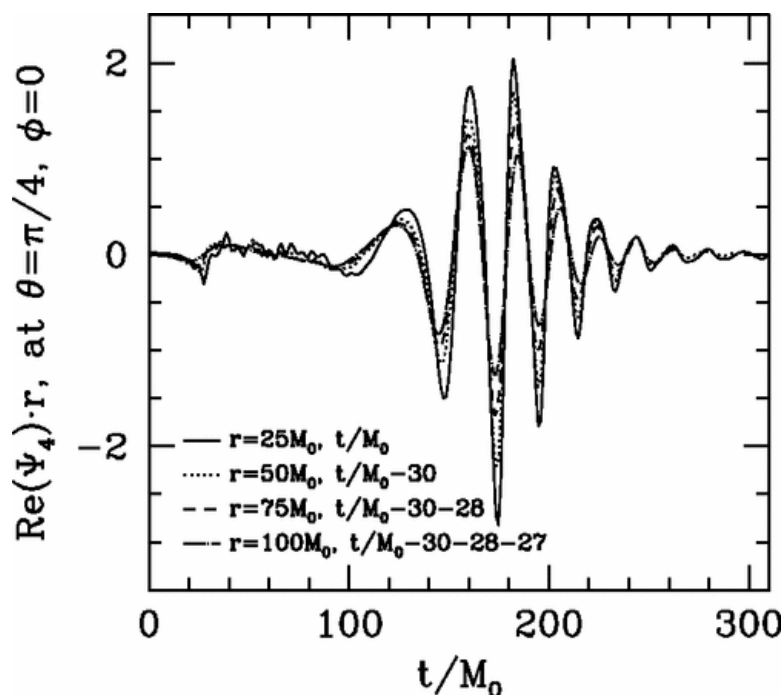
Fig 4.1: The first NR waveform, as presented in **Pretorius:2005gq**

Nowadays, it is the backbone of all other methods and is seen as the gold standard. Of course it remains very computationally expensive and making any sizable bank of purely NR waveforms fools endeavor. To date only a couple hundred parameter space points have been simulated. Thus NR is used to complement, calibrate and extend the other waveform generation techniques. For example to detect the first signals LIGO and others interpolated between parameter space points to reach the ones needed for detection. However, with the advent of LISA on the horizon, a further problem will arise. NR results by nature only take into account the last few orbit cycles before merger. Any more than that, and computational time becomes prohibitive. LISA with its low noise floor should be able to detect inspiraling but not yet merging binaries. To do so however will require waveform templates with hundreds of orbits, well out of reach from any modern NR package. Nonetheless, this technique has shown and will continue to show its worth, as no approximations other than discretization are made. The physical content of such waveforms is thus quite high.

4.2 Inspiral methods

Before continuing to the EOB method, let us look at the techniques that focus on the inspiral part of the waveform. There are broadly speaking three methods that fall in this category. The first we have already encountered at 1st order: PN. It is a perturbative expansion in both relative velocity (slow moving limit) and the coupling constant G (weak field limit) of the EFE. The second is the PM method, which is a perturbative expansion in *only* the coupling constant G. At face value the PM method contains the PN one as a special case, however as at zeroth order, the PM approximation capures straight line motion, and is generally more expressive of scattering. The final approximation can be applied when the mass ratio of the object in question is large. Here one can expand around a fixed but *not* flat mertric, essentially considering one of the objects as a test-particle evolving on a background caused by the heavier object. This is called the Gravitational Self-Force () formalism.

4.2.1 PN

The PN expansion, like its name suggests, is a perturbative expansion of EFE in the orbital regime, that at LO is given by tnewtonian gravity. Consider a system of orbiting bodies with typical values $\bar{M}, \bar{R}, \bar{v}$ for masses, separations, and velocties. Then the virial theorem states:

$$\langle T \rangle_\tau = -\tfrac{1}{2} \langle U \rangle \implies \bar{M}\bar{v}^2 \sim \frac{G\bar{M}^2}{\bar{R}} \qquad (4.1)$$

thus we can consider the following equivalent small parameters:

$$\bar{v}^2 \sim \frac{G\bar{M}}{\bar{R}}$$

We therefor expand in both velocities and coupling constant. This can be achieved with a by both a classical (albeit quite complicated) perturbative treatment [**Blanchet:2013haa**, **Blanchet:1995fg**], and a more contemporary EFT based approach called coyly NRGR [**Goldberger:2004jt**] as it was

inspired by Non-Relativistic Quantum Chromodynamics (). We call specific orders of the expansion nPM when the expansion is carried out to $\mathcal{O}(v^{2n})$.

Regardless of method, there are a few shortcomings with this expansion. While it is well suited to describe the *motion* of objects in an orbital regime, it is not well suited to describe gravitional radiation far from the source, as it exhibits divergences for $r \to \infty$[22]. This means that in the GW context, the PN expansion is in fact usually coupled to a weak-field approximation (see below), outside of the near zone. This is the region surrounding the source, that is of small extent compared to the wavelength of the emitted radiation:

$$r \ll \lambda \qquad (4.2)$$

The PN expansion can equally be viewed as an expansion in small 'retardations'. To see this consider that if the source is slowly moving, then the time derivatives of the metric generated by this source will be smaller than the spatial derivatives by a factor $\mathcal{O}(v)$,

$$\frac{\partial}{\partial t} = \mathcal{O}(v) \frac{\partial}{\partial x^i},$$

or $\partial_0 = \mathcal{O}(\epsilon))\partial_i$. Thus the d'Alembertian operator, applied to the metric, to lowest order becomes a Laplacian,

$$-\frac{1}{c^2}\frac{\partial^2}{\partial t^2} + \nabla^2 = \left[1 + O\left(\epsilon^2\right)\right]\nabla^2.$$

This means that retardation effects, due to the time derivative, are small corrections. In the PN expansion we are consequently trying to compute some quantity $F(t - r)$, such as a given component of the metric, which is intrinsically a function of retarded time $t_r = t - r$, from its expansion for small retardation r,

$$F(t_r) = F(t) - r\dot{F}(t) + \frac{r^2}{2}\ddot{F}(t) + ...$$

Now importantly the derivatives should bring down factors proportional to frequency Ω of the emitted radiation. Thus this is in fact an expansion in $r\Omega \sim r/\lambda$, and is thus only valid in the near zone as defined by 4.2, and breaks down

[22] in HEP speak this is an infrared divergence

outside of this zone, in the so called *radiation zone*. A serious consequence of this fact is that the pure, naive PN expansion is unable to account for outgoing or incoming radiation, and thus unable to describe isolated systems. This is where the PM expansion comes in.

4.2.2 PM

The PM expansion is a rather more straightforward weak field expansion of EFE, a perturbative expansion in the coupling constant G. It thus covers all orders in velocity of the PN expansion, at a specific G order. We usually call nPM the corresponding $\mathcal{O}(G^n)$ expansion. Historically, it was mainly seen as the radiation zone partner to the PN expansion, providing the propagatation of the waves up to the observer. In such combination, the PM expansion is solving the vacuum EFE. It is usally set up to compute the a version of the metric perturabation, that is exact:[23]

$$\mathsf{h}_{\mu\nu} = \sqrt{-g}g^{\mu\nu} - \eta^{\mu\nu}.$$

The PM expansion is then given as:

$$\sqrt{-g}g^{\mu\nu} = \eta^{\mu\nu} + G\mathsf{h}_1{}^{\mu\nu} + G^2\mathsf{h}_2{}^{\mu\nu} + ...$$

meaning that:

$$\mathsf{h}^{\mu\nu} = \sum_{n=1}^{\infty} G^n \mathsf{h}_n{}^{\mu\nu}.$$

The EFE for this metric perturbation, when imposing dedonder gauge (2.9) is given by:

$$\Box_{SR}\mathsf{h}^{\mu\nu} = -16\pi G \mathsf{h}^{\mu\nu}\tau^{\mu\nu}, \qquad (4.3)$$

where $\tau^{\mu\nu}$ is the effective energy momentum tensor given by:

$$\tau^{\mu\nu} = (-g)T^{\mu\nu} - \frac{1}{16\pi G}\Lambda^{\mu\nu}$$

where $\Lambda^{\mu\nu}$ is the result of putting all the nonlinear terms of the einstein tensor to the RHS. It is dependent on the metric

[23] we have used $h_{\mu\nu}$ to denote the linear perturbation, whereas $\mathsf{h}_{\mu\nu}$ is the all order metric perturbation.

and thus depends highly non-linearly on $\mathsf{h}_{\mu\nu}$. We can write it as:

$$\Lambda^{\mu\nu} = L^{\mu\nu}[\mathsf{h}, \mathsf{h}] + M^{\mu\nu}[\mathsf{h}, \mathsf{h}, \mathsf{h}] + N^{\mu\nu}[\mathsf{h}, \mathsf{h}, \mathsf{h}, \mathsf{h}] + \mathcal{O}(\mathsf{h}^5).$$

In a vaccuum 4.3 reduces to:

$$\Box_{SR}\mathsf{h}^{\mu\nu} = \Lambda^{\mu\nu},$$

which we can solve iteratively order by order:

$$\Box_{SR}\mathsf{h}_1{}^{\mu\nu} = 0,$$
$$\Box_{SR}\mathsf{h}_2{}^{\mu\nu} = L^{\mu\nu}[\mathsf{h}_1, \mathsf{h}_1],$$
$$\Box_{SR}\mathsf{h}_3{}^{\mu\nu} = M^{\mu\nu}[\mathsf{h}_1, \mathsf{h}_1, \mathsf{h}_1] + L^{\mu\nu}[\mathsf{h}_1, \mathsf{h}_2] + +L^{\mu\nu}[\mathsf{h}_2, \mathsf{h}_1]$$

This method can be supplemented by a multipolar expansion of the $\mathsf{h}_n{}^{\mu\nu}$, that are truncated to a specific order corresponding to the PM order we are interested in. This combined expansion was pioneered by **Bonnor:1959**, then formalised by **Thorne:1980ru**, and finally applied in this present context by **Blanchet:1986**.

In terms of source dynamics, it is more appropriate (and uniquely able) to describe inherently relativistic phenomena, like gravitional scattering. Due to being less restrictive than PN it is also relatively more difficult, as at higher orders one encounters intricate families of relativistic integrals. Note that we have in fact computed the 1PM approximation already, in the last chapter when we linearized the EFE. Higher orders are far more difficult, especially for sources such as BBH.

With the rise of amplitude techniques from high energy physics, both EFT and full theory results have been succesful in extracting previously unreachable orders. nthis is because such techniques are perfectly suited to compute relativistic scattering as they were devellopped for this specific task. We will see this in the next chapter.

4.3 EOB

The second main full waveform generation technique is the the effective one body (EOB) formalism. It was developped by **Buonanno:1998gg**, initially as a non-perturbative resumming of the PN expansion. It was later extended to include the merger and ringdown effects in **Buonanno:2000ef**. Thus it became the first full waveform generating technique to actually produce a waveform. It has gotten progressively more powerful, as the PN expansions have gotten better, and even more recently PM results have been included **Damour:2016gwp**. Additonally NR and EOB can be combined to produce a very accurate waveform, with less computional overhead than NR alone.

As it's name suggests, the EOB framework tries to combine all the previous data into a hamitonian describing the motion of a single body. The idea comes from Newtonian binaries where the method to solve the two body problem is to turn it into a one body problem. Further inspiration came from the two body problem in Quantum Electrodynamics () [**Brezin:1970zr**] .

Consider two bodies, with masses m_1 and m_2, positions $\mathbf{q}_1$, $\mathbf{q}_1$ and momenta $\mathbf{p_1}$ and $\mathbf{p_2}$ respectievly. The system can be described by the following hamiltonian:

$$\mathcal{H}_{\text{newton}}(\mathbf{q}_1, \mathbf{q}_1, \mathbf{p_1}, \mathbf{p_2}) = \frac{\mathbf{p_1}^2}{2m_1} + \frac{\mathbf{p_2}^2}{2m_2} - \frac{Gm_1 m_2}{|\mathbf{q_1} - \mathbf{q_1}|}$$

One then transforms this hamitionan into one descibing the relative motion $\mathbf{q} = \mathbf{q}_1 - \mathbf{q}_1$. One can formalise this by defining a new set of generalised coordinates, through a canonical transformation. We can even go further and employ a generating function for the transformation, ensuring that hamiton's equations stay unchanged (see **Goldstein:2002**). To descibe relative motion, we use jacobi coordinates $(\mathbf{Q}, \mathbf{q})$:

$$\begin{pmatrix} \mathbf{q}_1 \\ \mathbf{q}_1 \end{pmatrix} \rightarrow \underbrace{\begin{pmatrix} \frac{m_1}{M} & \frac{m_2}{M} \\ 1 & -1 \end{pmatrix}}_{A} \begin{pmatrix} \mathbf{q}_1 \\ \mathbf{q}_1 \end{pmatrix} = \begin{pmatrix} \mathbf{Q} \\ \mathbf{q} \end{pmatrix} \qquad (4.4)$$

If we now define the following generating function for the transformation, depending on the old positions coordinates $\mathbf{q}_i$ and the new momenta $\mathbf{P}_i$:

note the use of einstein summation

$$f_{II}(\mathbf{q}_i, \mathbf{P}_i) = \mathbf{P}_i A^{ij} \mathbf{q}_j \qquad (4.5)$$

Then the old momenta is given by:

$$\mathbf{p_i} = \frac{\partial f_{II}}{\partial \mathbf{q}_i} = \mathbf{P}_i A^{ij} \iff \mathbf{P}_i = [A^{-1}]^{ij} \mathbf{p_i} \qquad (4.6)$$

Where we can directly invert this equation and obtain the new momenta as:

$$\begin{pmatrix} \mathbf{P} \\ \mathbf{p} \end{pmatrix} = \begin{pmatrix} \mathbf{P}_1 \\ \mathbf{P}_2 \end{pmatrix} = \begin{pmatrix} 1 & 1 \\ \frac{m_2}{M} & -\frac{m_1}{M} \end{pmatrix} \begin{pmatrix} \mathbf{p_1} \\ \mathbf{p_2} \end{pmatrix}$$

Where as expected we obtain that one of the momenta descibes the center of mass momentum $\mathbf{P} = \mathbf{p_1} + \mathbf{p_2}$. The other positions are by constuction given by $\frac{\partial f_{II}}{\partial \mathbf{q}_1} = \mathbf{Q}$ and $\frac{\partial f_{II}}{\partial \mathbf{q}_1} = \mathbf{q}$ i.e the same as equation 4.4. Finally the new hamiltonian $\mathcal{H}_{\rm rel}(\mathbf{Q}, \mathbf{q}, \mathbf{P}, \mathbf{p})$ can be directly obtained by the generating function:[24]

$$\mathcal{H}_{\rm rel}(\mathbf{Q}, \mathbf{q}, \mathbf{P}, \mathbf{p}) = \mathcal{H}_{\rm newton}(\mathbf{Q}, \mathbf{q}, \mathbf{P}, \mathbf{p}) + \cancelto{0}{\frac{\partial f_{II}}{\partial t}} = \frac{\mathbf{P}^2}{2M} + \frac{\mathbf{p}^2}{2\mu} - \frac{Gm_1 m_2}{|\mathbf{q}|}$$

Where $M = m_1 + m_2$ is the total mass, and $\mu = \frac{m_1 m_2}{M}$ is the reduced mass. If we move to a frame where the $\mathbf{Q}$ is at rest, i.e. $\mathbf{P} = 0$ the hamiltonian colapses to a one body hamiltonian. The two-body problem we started with has can now be though of as the one body problem of a test-particle of mass μ orbiting an external mass M.

The EOB framework takes the above derivation and generalises it to general relativity. The defining trick used above is to transform to 'better' coordinates. A first step is to demand that for straight line motion the Center of Momentum () energy $E_{\rm COM} = P^0$, where P it the 4-momentum of the entire-system, is equal to the hamiltonian. We have then:[25]

$$\mathcal{H} = \sqrt{M^2(1 + 2\nu(\gamma - 1))}$$

[24] We just plug in the definition of the old momenta in terms of the new (4.6):

$$\mathbf{p_1} = \frac{m_1}{M}\mathbf{P} + \mathbf{p}$$
$$\mathbf{p_2} = \frac{m_2}{M}\mathbf{P} - \mathbf{p}$$

[25] In the COM frame, the spacial part of the total momentum is zero (by defintion), and thus we have:

$$P_0^2 = P^2 = (p_1 + p_2)^2 = p_1^2 + p_2^2 + 2p_1 \cdot p_2$$

Where $\nu = \frac{\mu}{M}$ is the symmetric mass ratio, and $\gamma = \frac{1}{\sqrt{1-v^2}} = \frac{p_1{}^\mu p_{2\mu}}{m_1 m_2}$ is the relative lorentz-factor. Note that for noninteracting systems we have $p_\mu p^\mu = \mu^2$ and we can call the effective hamitonian:

$$\mathcal{H}_{\text{eff}} = p^0 = \sqrt{\mu^2 + \mathbf{p}^2} = \mu\gamma \qquad (4.7)$$

And then we can substitute this into the hamiltonian above, and add back a generic system momentum $\mathbf{P}$ and obtain:

$$\mathcal{H}_{\text{eob}} = \sqrt{M^2(1 + 2\nu(\frac{\mathcal{H}_{\text{eff}}}{\mu} - 1)) + \mathbf{P}^2}$$

This Hamiltonian (with $\mathcal{H}_{\text{eff}}$ given by 4.7) now describes straight line motion in a relativistic framework. The key point is that we can take $\mathcal{H}_{\text{eff}}$ to be a gravitational test mass Hamiltonian, with some specific deformations and this will match the PN result. Consider a test mass in a schwarzschild background 2.27, i.e. we consider the case of non spinnning black holes. We can start from the reduced-mass shell expression:

$$g^{\mu\nu}p^\mu p^\nu = -\mu^2 \qquad (4.8)$$

where $g^{\mu\nu}$ is given by 2.27, where we can set $\theta = \frac{1}{2}\pi$ to fix the orientation[26]. Just as before the effective hamiltonian is the 0th component of the momentum, which is implicitly given by 4.8:

$$\mathcal{H}_S = \sqrt{A_S(\mu^2 + A_S p_r^2 + \frac{L^2}{r^2})},$$

where $A_S = \frac{1}{1 - R_S/r}$, and $L = p_\phi$ is the angular momentum. We then allow deformations from this hamiltionian defining:

$$\mathcal{H}_{\text{eff}}(r, p_r, phi, L) = \sqrt{A(\mu^2 + A\bar{D}p_r^2 + \frac{L^2}{r^2}) + Q},$$

where $A, \bar{D}, Q$ are the so-called EOB potentials. $A, \bar{D}$ correspond to the radial potentials of the effective metric, while Q contains terms quadratic in the momentum. We can then match these to PN reslults, by matching observables.

[26] this is always possible through a change of variables

This is more than a neat trick as this Hamiltonian when well-matched fits the gold standard NR result up to the merger, well out of the PN regime. Crucially this Hamiltonian framework does not take into account radiation reaction by construction (since it is based on conserved energy). These dissipative effects are rather added after the fact, as friction terms in the EOM. The normal conservative eom is straightforwardly obtained through Hamiltions equations:

$$\dot{r} = \frac{\partial \mathcal{H}_{\text{eff}}}{\partial p_r}, \quad \dot{p}_r = -\frac{\partial \mathcal{H}_{\text{eff}}}{\partial r}$$

$$\omega = \dot{\phi} = \frac{\partial \mathcal{H}_{\text{eff}}}{\partial L}, \quad \dot{L} = -\frac{\partial \mathcal{H}_{\text{eff}}}{\partial \phi}\overset{0}{\diagup}.$$

Note that as expected the angular momentum is conserved. We will now spoil this conservation, add friction forces, so called radiation reaction forces to the changes in momentum (radial and angular):

$$\dot{p}_r = -\frac{\partial \mathcal{H}_{\text{eff}}}{\partial r} + f_r$$

$$\dot{L} = f_\phi.$$

Now we can express the energy loss:

$$\dot{E} = \frac{\mathrm{d}\mathcal{H}_{\text{eff}}}{\mathrm{d}t} = \frac{\partial \mathcal{H}_{\text{eff}}}{\partial r}\dot{r} + \frac{\partial \mathcal{H}_{\text{eff}}}{\partial p_r}\dot{p}_r + \frac{\partial \mathcal{H}_{\text{eff}}}{\partial L}\dot{L} = f_r\dot{r} + f_\phi\omega.$$

We can now account for such dissipative effects by matching to PN results for the angular momentum flux, and the energy flux given by the so called balance laws:

$$\langle \mathcal{F}_L \rangle = -\langle \dot{L} \rangle = -\langle f_\phi \rangle,$$
$$\langle \mathcal{F}_E \rangle = -\langle \dot{E} \rangle = -\langle f_r\dot{r} + f_\phi\omega \rangle.$$

With this we obtain as full of a picture of the inspiral as possible given the inputs, namely PN. The matching can also be done with PM and NR results, further increasing the validity and precision of EOB. Of course we are still missing the merger and ringdown. The merger, or plunge was

predicted in **Buonanno:2000ef** to be simply the peak in the waveform. This waveform is conected smoothly to a ringdown waveform, defined by a sum of quasi -normal modes of the remnant after merger. Thus one obtains a sort of frankenstein waveform, pooling resources from PN, PM, NR and black hole perturbation theory. Importantly, when well matched, this waveform is almost as accurate as NR results, but with the added benefit of being able to be computed in a reasonable amount of time. Of course it is still only as powerful as the inputs tow which we match, namely the PN or PM results. We will explore how to compute PM results using amplitudes in the next section.

5 Scattering amplitudes and GWs

Whilst we have almost no hope to detect any GW scattering events with current experiments, scattering calculations can still be very useful in the quest for orbital waveforms. Most importantly, while experimental data is not driving gravitational scattering theory, particle scattering experiment and theory have been an enormously fruitful endeavor for High energy physics. The back and forth between precise measurements (such as those conducted at the Large Hadron Collider ()) and precise predictions for particle scattering, has pushed the boundaries of the calculations possible. It would be therefore very beneficial if one could apply the large knowledge acquired for small non-gravitationally interacting particles, to large compact orbiting bodies.

Such techniques as EFT, double copy, generalized unitarity, Integration by Parts () reduction, differential equations methods, all standing on the shoulders of Feynman perturbative techniques have been applied to the scattering problem in gravity. A key part of applying tools originally developed for mostly quantum systems is controlling the classical limit, and is part of the solution to implementing gravity in a QFT framework, a historically difficult endeavor. Once scattering data is obtained one needs to extract the relevant observables. This may be in an effort to compare results from the different methods, in which case gauge and diffeomorphism invariance are key. It can also be to extract the relevant information for detection and data extraction, in which case the GW waveform is the relevant observable. In the latter case one is mostly interested in the orbital waveform, and thus a map from unbound to bound orbits is necessary.

Multiple formalisms have arisen to map the scattering problem to an orbital one, and the quantum formalism to a classical one. One key way is to map scattering data to the potential (as present in a Hamiltonian for example).

In fact this has been developped as early as the 1970s in [**Hiida:1972xs**, **Iwasaki:1971vb**]. Further developments happened in [**Neill:2013wsa**, **Bjerrum-Bohr:2013bxa**, **Vaidya:2014kza**, **Cachazo:2017jef**, **Guevara:2017csg**, **Damour:2016gwp**]. Here we will follow the treatment in **Cheung:2018wkq**, where one uses the conservative part of such scattering amplitudes to match to an EFT and subsequently to map to the potential. Recently efforts to add disipative effects have been succesful aswell [**Kalin:2022hph**]. This potential can then be used as input to the EOB formalism. Furthermore, **Kalin:2019rwq**; **Kalin:2019inp**, have shown a path forward in directly extending unbound data to bound orbits, obviating the need to use a potential and EOB at all.

Finally as mentioned in the last chapter, scattering can stand on its own and is still usefull, unextended to the orbital case. The PM approximation can be computed from scattering amplitudes in an EFT framework [**Kalin:2020mvi**]. We can also explore the classical observables possible in scattering scenarios. This has been developed in **Kosower:2018adc** and was extended to local observables[27] such as waveforms in **Cristofoli:2021vyo**.

In this chapter we will first look at how one uses amplitude data to extract orbital and scattering waveforms. We will then look at the KMOC formalism to directly extract observables. Finally we will look at obtaining these amplitudes, combining all the methods and comparing to results such as those in [**Kosower:2018adc**, **Bern:2021xze**].

5.1 Scattering amplitudes

In QFT one way to encode scattering data is through a scattering amplitude. Consider a process where one starts out with a set of particles described by a state $|i\rangle$, we let them interact, and end up with a final state $|f\rangle$. The scattering amplitude is then defined as the probability amplitude for this process to occur. It is simply given by

$$\langle i|S-1|f\rangle = (2\pi)^4 \delta^{(4)}(p_f - p_i)i\mathcal{A}_{fi},$$

where S is essentially the operator that 'does the scattering'. We subtract the identity from it, forming what some call the

[27] local as in not time integrated and thus presenting time dependent dynamics

transfer matrix T as we only are interested in processes where something happens (i.e. not everything stays the same). In the above equation we also define the *scattering matrix element* $\mathcal{A}_{fi}$ [**Srednicki:2007**] or *invariant Feynman amplitude* [**Coleman:2018**], by factoring out a normalised spacetime delta-function imposing conservation of momentum on the external fields, and a complex unit. The key point is that this amplitude can be computed using graphical techniques. This makes use of the Lehmann Symanzik and Zimmermann () [**Lehmann:1954rq**, **Collins:2019ozc**] formalism where such an amplitude $\mathcal{A}_{fi}$, can be computed from products of time ordered correlation functions of the given QFT. These are also called Green's functions, which can then be encoded by sums of Feynman diagrams. The diagrams are generated by applying Feynman rules which can be readily obtained from an action describing the theory. This technique will be exemplified in the following sections.

5.2 From amplitude to potential

Let us now look at how to map the amplitude to the gravitational potential, for use in the EOB formalism. We will follow the treatment in **Cheung:2018wkq**. We first start with defining the effective theory that describes our problem as two scalar fields f_1 and f_2 with masses m_1 and m_2 interacting through a long range potential $V(r)$. It is simply the EFT for non-relativistic fields. This EFT is described by the following action:

$$S = \int \mathrm{d}t\, \mathcal{L}_{\mathrm{kin}} + \mathcal{L}_{\mathrm{int}},$$

where the kinetic term is given by:

$$
\begin{aligned}
\mathcal{L}_{\mathrm{kin}} = &\int \tilde{\mathrm{d}}^{D-1}\mathbf{k}\, f^*_{\,1}(-\mathbf{k})\Big(\mathring{i}\partial_t - \sqrt{\mathbf{k}^2 + m_1}\Big)f_1(\mathbf{k}) \\
&+ \int \tilde{\mathrm{d}}^{D-1}\mathbf{k}\, f^*_{\,2}(-\mathbf{k})\Big(\mathring{i}\partial_t - \sqrt{\mathbf{k}^2 + m_2}\Big)f_2(\mathbf{k})
\end{aligned}
$$

and the interaction term is given by:

$$\mathcal{L}_{\text{int}} = -\int \tilde{\mathrm{d}}^{D-1}\mathbf{k}\ \tilde{\mathrm{d}}^{D-1}\mathbf{k}'\ V(\mathbf{k}, \mathbf{k}') f^*_{\ 1}(\mathbf{k}') f^*_{\ 2}(-\mathbf{k}') f_1(\mathbf{k}) f_2(-\mathbf{k}).$$

This theory is obtained from the full one by integrating out all the massless force carriers , which are consequently encoded in the potential $V(\mathbf{k}, \mathbf{k}')$ and taking the non-relativistic limit $|\mathbf{k}|, |\mathbf{k}'| \ll m_{1,2}$. In a classical system we consider the particles to be separated by a minimum distance, called impact parameter $|\mathbf{b}|$, and consider that their compton wavelength $\ell_c \sim \frac{1}{|\mathbf{k}|}, \frac{1}{|\mathbf{k}'|}$[28] is much smaller than this separation:

[28] note the use of natural units

$$|\mathbf{b}| \ll \ell_c \simeq \frac{1}{|\mathbf{k}|}, \frac{1}{|\mathbf{k}'|}$$

This ensures that the particles are not interacting quantum mechanically in any significant way. Interestingly this heirachy of scales can be rewritten as:

$$\mathbf{J} \sim |\mathbf{k} \times \mathbf{b}| \gg 1$$

Thus any two body classical system has large angular momentum. We can thus extract the classical part of any quantity by taking the LO contribution in the inverse of angular momentum, or equivalently:

$$\frac{1}{J} \propto \frac{1}{|b|} \sim |\mathbf{k} - \mathbf{k}'| \propto \frac{1}{\kappa} \tag{5.1}$$

Where we used in the first step that angular momentum is proportional to separation. We then applied the fact that in scattering scenarios the impact parameter is proportional to the inverse of the momentum transfer $\sim \frac{1}{|\mathbf{q}|}$ where :

$$q = (0, \mathbf{q}) = (0, \mathbf{k} - \mathbf{k}').$$

The last relation in 5.1 holds due to the virial theorem. Where κ is the coupling constant, which in the case of gravity is $\kappa = 4\pi G$. Since the potential must encode the coulomb

potential $\kappa/|\mathbf{k} - \mathbf{k}'|^2 \propto J^3$, it must scale similarly. We thus formulate the following ansatz for the potential:

$$V(\mathbf{k}, \mathbf{k}') = \sum_{n=0}^{\infty} \frac{\kappa^n}{|\mathbf{k} - \mathbf{k}'|^{D-1-n}} c_n \left(\frac{\mathbf{k}^2 + \mathbf{k}'^2}{2} \right) \qquad (5.2)$$

Note that higher order terms in the potential could be formed by any combination of momentum invariants $\mathbf{k}^2$, $\mathbf{k}'^2$, and $\mathbf{k} \cdot \mathbf{k}'$, however not all combinations of these are independent. The ansatz is chosen such that only the combination $|\mathbf{k} - \mathbf{k}'|$ and $\mathbf{k}^2 + \mathbf{k}'^2$ is present, the others being combinations reachable by field redefinition, or vanishing on-shell, such as $\mathbf{k}^2 - \mathbf{k}'^2$. Note as-well that we work in $D = 4 - 2\epsilon$ dimensions such that the integrals are dimensionally regulated [**tHooft:1972tcz**]. This means that an ϵ-power corresponds to a logarithm[29].Finally note that in gravity this is precisely a PM expansion!

[29] the third term in the sum is given by $\kappa^3 \ln(\mathbf{k} - \mathbf{k}')^2 c_3 \left(\frac{1}{2}\mathbf{k}^2 + \mathbf{k}'^2 \right)$

5.2.1 EFT amplitude

The first step in establishing a link to the potential from a generic scattering amplitude computed in the full theory is to compute the amplitude in the EFT. We first identitify the Feynman rules from the action. The kinetic term encodes the propagator:

$$\xrightarrow{(k_0, \mathbf{k})} \quad = \quad \frac{\mathring{i}}{k_0 - \sqrt{\mathbf{k}^2 + m_{1,2}^2} + \mathring{i}0}$$

Propagator rule

where the $\mathring{i}0$ is the Feynman prescription for avoiding the poles. The interaction term encodes the vertex:

$$\mathbf{k} \; \mathbf{k}' \quad = \quad \mathring{i} V(\mathbf{k}, \mathbf{k}')$$
$$-\mathbf{k} \; -\mathbf{k}'$$

Vertex rule

The key point is that the EFT amplitude for two-to-two scattering must be equal to the full amplitude at every order

46

in the coupling constant κ. The expression for the EFT amplitude will contain the coefficient functions from 5.2 since they will be present as vertex terms. Particle number must be conserved in the non-relativistic limit [30], so the amplitude is a sum of bubble diagrams:

[30] as pair production is kinematically forbidden

$$\mathcal{A}_{\text{EFT}} \; = \; \cdots$$

EFT amplitude

We can consequently neatly organise the amplitude into a sum of terms with specific loop counts. We can also equivalently organise it into a sum of terms with specific κ powers. We write,

$$\mathcal{A}_{\text{EFT}} = \sum_{L=0}^{\infty} \mathcal{A}_{\text{EFT}}^{L\text{loop}} = \sum_{i=1}^{\infty} \mathcal{A}_{\text{EFT}}^{(i)}.$$

Notably, these partitions do not line up for the EFT since the vertex contains all powers of the coupling. This is in contrast to the full theory where usually they yield the same partition. We will eventually want to partition over the coupling power to compare the full theory.

Since every vertex has degree 4, and we have two scalars in and two scalars out, it is convient to define a 2-body propagator. We can already integrate over the energy component of the loop momentum, since the vertex does not have an energy dependence:[31]

[31] the 4-momentum conservation at each vertex means that the energy components of the two propagating momenta must carry along the energy component of the initial state. This can be encoded by demanding that $\omega_1 + \omega_2 = E$. Taking the COM frame for the intial momenta means that the 3 momenta of each propagator must cancel i.e. $\mathbf{k}_1 + \mathbf{k}_2$

$$\mathring{\imath}\Delta_2(\mathbf{k}) = \int \tilde{\mathrm{d}}\omega \, \frac{\mathring{\imath}}{\omega - \sqrt{\mathbf{k}^2 + m_1^2}} \frac{\mathring{\imath}}{E - \omega - \sqrt{\mathbf{k}^2 + m_2^2}} = \frac{\mathring{\imath}}{E - \sqrt{\mathbf{k}^2 + m_1^2} - \sqrt{\mathbf{k}^2 + m_2^2}},$$

where the integral is performed using the residue theorem, closing the contour in either half plane, where in either case a pole is present. Note that we define $E = E_1 + E_2$ to be the COM energy of the two inital states:[32]

[32] which is equal to the outgoing energy

$$E_{1,2} = \sqrt{\mathbf{p}^2 + m_{1,2}^2} = \sqrt{\mathbf{p'}^2 + m_{1,2}^2},$$

where $\mathbf{p}$ and $\mathbf{p}'$ are the initial and final three-momenta of the two states [33] in the COM frame. Finally we can write what the diagram at loop level $L > 0$ encodes:

[33] for example in the initial state one scalar field will have 3-momentum $\mathbf{p}$, and the other $-\mathbf{p}$

$$\mathcal{A}_{\text{EFT}}^{L\text{loop}} = \int \prod_{i=1}^{L} \tilde{\text{d}}^{D-1}\mathbf{k}_i \, V(\mathbf{p}, \mathbf{k}_1)\Delta_2(\mathbf{k}_1)\cdots\Delta_2(\mathbf{k}_L)V(\mathbf{k}_L, \mathbf{p}').$$

This integral can be perfomed in the non-relativistic limit, as done by **Bern:2019crd** up to 3PM, using IBP reduction yielding, up to 2PM, the amplitudes of the EFT:[34]

[34] here the repartioning mentioned above has been applied and a change in loop momenta: $\mathbf{k}_i \to \mathbf{p} + {}_i$

$$\mathcal{A}_{\text{EFT}}^{(1)} = -\frac{4\pi G c_1}{\mathbf{q}^2}$$

$$\mathcal{A}_{\text{EFT}}^{(2)} = \pi^2 G^2 \Big(-\frac{2c_2}{|\mathbf{q}|} + \frac{1}{E\xi|\mathbf{q}|}\Big[(1-3\xi)c_1^2 + 4\xi^2 E^2 c_1 c_1'\Big]$$
$$\int \tilde{\text{d}}^{D-1} \frac{32E\xi c_1^2}{{}^2(\mathbf{q} +)^2({}^2 + 2\mathbf{p})}\Big),$$

where $\xi = \frac{E_1 E_2}{(E_1+E_2)^2}$ is the reduced energy ratio. The arguments of the coefficent functions c_1 are kept iplicit and a prime denotes a derivative with respect to $\mathbf{p}$. Additionally we define $\mathbf{q} = \mathbf{p}' - \mathbf{p}$ to be the 3-momentum transfer. Now provided we obtain the amplitude of the full theory, and carefully apply the same limiting procedures, we have that

$$\mathcal{A}_{\text{EFT}}^{(i)} = \mathcal{A}_{\text{full}}^{(i)} \quad \forall i.$$

This enables us to fix the coefficients in the potential ansatz 5.2, and fullfils the promised map from amplitude to potential. Importantly we must apply the limiting procedure applied above, i.e. the classical and non relativitic limit. We can summarise this by setting the following heirarchy:

$$m_1, m_2 \ll J|\mathbf{q}| \ll |\mathbf{q}|.$$

For the full theory this can be encoded as restricting to a specific kinematic regime, following the method of regions. We consider all the possible loop-momentum scalings, first due to the classical limit:

Region	Momentum $\ell = (\omega,)$
hard	(m, m)
soft	$(|\mathbf{q}|, |\mathbf{q}|)$

The soft region is responsible for the classical limit in this language, as we consider a small $|\mathbf{q}|$ expansion. We will infact explore this fact in a different light in Section 5.3. Taking the NR limit corresponds to a subregion of the soft region, the so-called potential region:

$$(\omega,) \sim (|\mathbf{q}|, |\mathbf{q}|),$$

where we use that the NR expansion is a given by

$$|\mathbf{p}| \ll m$$

and thus equivalently[35] by a small relative velocity:

$$|\mathbf{u}| \ll 1.$$

[35] dividing by mass

To summarise, to obtain the form of the potential, we first compute the amplitude in an EFT, absorbing all force carrying particles into an effective vertex. Making an ansatz for the potential we can go ahead and compute this amplitude in the non-relativistic limit. This same amplitude can be computed in the full theory, but by still taking the limiting procedure we drastically reduce the kinematic region, simplifying calculations (in fact eliminating diagrams) and allowing us to match order by order the EFT amplitude. This fixes the coeffecents postulated for the potential.

Unfortunately the procedure desribed above, and in fact *any* procedure trying to make contact with EOB through expanding the gravitiational potential, automatically does not capture the full physics. The crucial point that makes compact binaries interesting is that they are not isolated, energy conserving systems. The energy of the system is lost to the gravitational waves that enable us to detect them. Any conservative dynamics, by construction, cannot capture this loss of energy. In the context of EOB this radiation reaction was added after the fact, through direct modifications of the EOMs obtained from Hamilton's equations. It is not clear

how to incorporate dissipative data from the amplitude in the EOB framework.

One way to not encounter this difficulty is to full bypass the EOB framework and try to obtain observables directly from the amplitude. This is the subject of the following sections.

5.3 KMOC

The setup of the KMOC framework (**Kosower:2018adc**) is very general, and is aimed at taking the classical limit of a scattering event in an unspecified theory. We will later on apply it to Scalar Quantum Electrodynamics () and gravity.

First let us define our conventions. Throughout this section we use relativistically natural units, i.e. we do *not* set $\hbar = 1$. This will essentially be the small parameter that multiplies the soft momenta, that defined the region in Section 5.2. In this section we will further motivate this classical limit, in more detail, by taking the generally accepted limit that makes quantum physics collapse to classical physics:

$$\hbar \to 0.$$

We still retain $c = 1$, meaning that, using dimensional analysis we have that $[L][T]^{-1} = 1 \implies [L] = [T]$, length and time are measured in the same units. Correspondingly, energy is measured in units of mass:

$$E = mc^2 \implies [E] = [m] = [M]$$

and $\hbar$ has the following units:

$$E = \hbar\omega \implies [M] = [\hbar][T]^{-1} \implies [\hbar] = [T][M].$$

Thus momentum p has units of $[p] = [M]$ mass and Wavenumber $[\bar{p}] = [\frac{p}{\hbar}] = [T]^{-1}$ has units of inverse time. We will denote the on-mass-m-shell measure by $\mathrm{d}\Phi(p)$ [36]:

$$\int \mathrm{d}\Phi(p) \cdots = \int \frac{\mathrm{d}^3\mathbf{p}}{2\hbar\omega_{\mathbf{p}}(2\pi)^3} \cdots = \int \tilde{\mathrm{d}}^4 p\, \tilde{\delta}^{(+)}(p^2 - m^2) \cdots,$$

[36] Repeated integration will be denoted $\mathrm{d}\Phi_n(p_1, \ldots, p_n)$

50

where quantities denoted by bars absorb the relevant factors of 2π, such that $\tilde{\mathrm{d}}^n p = \frac{\mathrm{d}^n p}{(2\pi)^n}$. Additionally we have defined $\hbar\omega_{\mathbf{p}} = \sqrt{\mathbf{p}^2 + m^2}$ to be the on-shell energy and $\delta^{(+)}$ is the normalised positive energy on-shell delta function:

$$\tilde{\delta}^{(+)}(p^2 - m^2) = (2\pi)\delta(p^2 - m^2)\Theta(p^0) = \tilde{\delta}(p^2 - m^2)\Theta(p^0)$$

With our conventions at hand, let us set the stage for the problem. Imagine we want to scatter two particles, be they massive black holes, or tiny electrons into each other, with a constant particle number (i.e. a classical two in two out scattering). As mentioned in Section 5.1, in QFT the framework that formalizes scattering of definite particle number states is called the LSZ reduction.

Let us look at it in more detail. The first component is to define the states we want to scatter. Suppose our theory has single particle states $|p\rangle$, with mass m, eigenstates of the momentum:

$$\mathbb{P}^\mu |p\rangle = p^\mu |p\rangle \quad \text{where} \quad p^0 = \hbar\omega_{\mathbf{p}} = \sqrt{\mathbf{p}^2 + m^2}.$$

These states can be seen as special cases (the plane wave states) of wavepacket states:[37]

$$|f\rangle = \int \mathrm{d}\Phi(k)\, \check{f}(k)|k\rangle,$$

where $\check{f}(k)$ is the momentum space wavefunction or more mathematically the momentum distribution function. Note that it is almost a fourier transform, but not quite, as it is performed on mass shell. If the spacetime 'wavefunction' [38] is given by:

$$f(x) = \int \mathrm{d}\Phi(k)\, \check{f}(k)\mathrm{e}^{-ik\cdot x}, \tag{5.3}$$

the $\check{f}(k)$ is consequently given by:

$$\langle k|f\rangle = \check{f}(k) = 2\hbar\omega_{\mathbf{p}} \int \mathrm{d}^3\mathbf{x}\, f(x)\mathrm{e}^{ik\cdot x}. \tag{5.4}$$

we work in the Heisenberg picture here

[37] A plane wave state $|f\rangle = |p\rangle$ would be given by $\check{f}(k) = 2\hbar\omega_{\mathbf{k}}\tilde{\delta}^{(3)}(\mathbf{k} - \mathbf{p})$

[38] Note that the concept of coordinate space wavefunction is ill defined in interacting theories. However for such asymptotic states, the wavefunction outside the bulk (on the infinte time boundary) is that of a free wavefunction

If we now define the following operators:[39]

$$a_f^\dagger(t) = -\mathring{\imath} \int \mathrm{d}^3\mathbf{x}\, f(x) \overleftrightarrow{\partial_0} \phi(x)$$

$$a_f(t) = \mathring{\imath} \int \mathrm{d}^3\mathbf{x}\, f^*(x) \overleftrightarrow{\partial_0} \phi(x)$$

where $\phi(x)$ is the Heisenberg field operator of our theory. Note that while these operators are time dependent, this dependence is not given by applying the Heisenberg EOMs [40], instead it is present through the time dependence of the wavefunction $f(x)$. It turns out that these operators, suggestively written are the true creation and annihilation operators in the interacting theory.

Now we can actually define a general one particle state $|f\rangle$ as the result of a creation operator acting on the physical vacuum. Crucially however this only makes sense in the boundary of the bulk, i.e. at asymptotic times $t \to \pm\infty$[41]. Inside the bulk, any thusly created state would infact not have definite particle number. This definitely makes sense in the scattering problem because if you consider the whole system as a state, it only has definite particle number at asymptotic times, and inside the bulk the scattering happens, and the particle number is not conserved (at least quantum mechanically).

Consequently we only define asymptotic states, denoting them by an in subscript if they were created at $t \to -\infty$ and out if they were created at $t \to +\infty$. Thus we define a generic single particle in state as:

$$|f\rangle_{\mathrm{in}} \overset{\mathrm{def}}{=} \lim_{t \to -\infty} a_f^\dagger(t)|\Omega\rangle = a_{f;\mathrm{in}}^\dagger|\Omega\rangle = \int \mathrm{d}\Phi(k)\, \check{f}(k) \underbrace{a_\mathbf{k}^\dagger|\Omega\rangle}_{|k\rangle}$$

and the corresponding $t \to +\infty$ state where in is replaced with out. It turns out that the extension to multiparticle states is not much more complicated. The one thing to demand is that the momentum distributions say $\check{f}_1, \check{f}_2, \ldots$ have no common support, i.e. they are not overlapping. In this case a n-particle in state is defined as:

[39] $f\overleftrightarrow{\partial_\mu}g = f(\partial_\mu g) - (\partial_\mu f)g$

Note that if we replace $f(x)$ by a plane wave state $\mathrm{e}^{-\mathring{\imath}k \cdot x}$ we obtain and define the following:

$$a_\mathbf{k}^\dagger(t) = \int \mathrm{d}^3\mathbf{x}\, \mathrm{e}^{-\mathring{\imath}k \cdot x}\left[\hbar\omega_\mathbf{k} f(x) - \mathring{\imath}\partial_0 f(x)\right]$$

[40] $\frac{\mathrm{d}A_H(t)}{\mathrm{d}t} = \mathring{\imath}[H; A_H(t)]$ ... $\left[\hbar\omega_\mathbf{k} f(x) + \mathring{\imath}\partial_0 f(x)\right]$

[41] see **Coleman:2018** or **Collins:2019ozc** for a more in depth discussion of this point

$$|f_1, \dots, f_n\rangle_{\mathrm{in}} \stackrel{\mathrm{def}}{=} a^\dagger_{f_1;\mathrm{in}} a^\dagger_{f_2;\mathrm{in}} \dots a^\dagger_{f_n;\mathrm{in}} |\Omega\rangle = \int \mathrm{d}\Phi_n(k_1, \dots, k_n) \, \check{f}_1(k_1) \dots \check{f}_n(k_n) |k_1, \dots, k_n\rangle.$$

We now have the definitions for asymptotic in and out states for any number of particles. Before continuing to define the setup to scatter our two particles, let us look at the meaning of the position space wavefunction $f(x)$ as defined in 5.3. Consider a sharply peaked, compactly supported momentum distribution $\check{f}(k)$ around a value $\mathbf{p}_0$ and a characteristic width Δp. One such function could be:

$$f(\mathbf{p}; \mathbf{p}_0, \Delta p) = \begin{cases} N\mathrm{e}^{-1/(1-|\mathbf{p}-\mathbf{p}_0|^2/\Delta p^2)} & \text{if } |\mathbf{p}_0 - \mathbf{p}| < \Delta p \\ 0 & \text{if } |\mathbf{p}_0 - \mathbf{p}| \ge \Delta p \end{cases}, \tag{5.5}$$

where N is a normalization constant. Now the integrand in 5.3, at large t or $\mathbf{x}$, will be dominated by the stationary phase point $\mathbf{p}_s$ which is given by:[42]

$$0 = -\frac{\partial}{\partial \mathbf{p}_s}(\hbar \omega_{\mathbf{p}_s} t + \mathbf{p}_s \cdot \mathbf{x}) = -\frac{\mathbf{p}_s t}{\hbar \omega_{\mathbf{p}_s}} + \mathbf{x}. \tag{5.6}$$

In the case of a sharply peaked momentum distribution, the coordinate space wavefunction will be largest when the stationary phase point is be the same as the peak of the momentum distribution, i.e. $\mathbf{p}_s = \mathbf{p}_0$ i.e. substituting $\mathbf{p}_s$ into 5.6 gives:

$$\mathbf{x} \simeq \frac{\mathbf{p}_0 t}{\hbar \omega_{\mathbf{p}_0}} = \mathbf{v}_0 t.$$

This is precisely the trajectory of the classical relativistic particle. If we have two particles with different peaked momentum distributions their trajectories will have different velocities, but the same positions at time 0. Thus we will shift one of these trajectories by a so called impact parameter b^μ[43], parametrising the relative separtation of the two particles/wavepackets. This can be simply done by multiplying the momentum distribution $\check{f}_1(p)$ by a factor of $\mathrm{e}^{\frac{i}{\hbar}b \cdot p}$. We take it to be perpendicular to the initial momenta p_1, p_2. We now can write down the initial state that we are going to study:

[42] This then means that

$$\mathbf{p}_s = \frac{m\mathbf{x}\,\mathrm{sign}(t)}{\sqrt{t^2 - \mathbf{x}^2}}$$

thus

$$\hbar \omega_{\mathbf{p}_s} = \frac{m|t|}{\sqrt{t^2 - \mathbf{x}^2}}$$

[43] $f(x) = \int \mathrm{d}\Phi(p)\, \check{f}(p) \mathrm{e}^{-\frac{i}{\hbar} p^\mu x_\mu}$. Then a shifted, i.e. translated version of $f(x)$ can be written:

$$f(x - x_0) = \int \mathrm{d}\Phi(p)\, \check{f}(p)\, \mathrm{e}^{-\frac{i}{\hbar} p_\mu(x^\mu - x_0^\mu)}$$

$$= \int \mathrm{d}\Phi(p)\, \check{f}(p)\, \mathrm{e}^{\frac{i}{\hbar} p_\mu x_0^\mu}\, \mathrm{e}^{-\frac{i}{\hbar} p_\mu x^\mu}$$

Thus the associated, translated state is:

$$|f\rangle = \int \mathrm{d}\Phi(p)\, \check{f}(p)\, \mathrm{e}^{\frac{i}{\hbar} p_\mu x_0^\mu} |p\rangle$$

$$|\text{in}\rangle = \int d\Phi_2(p_1, p_2)\, \breve{f}_1(p_1)\breve{f}_2(p_2)e^{\frac{i}{\hbar}b_\mu p_1{}^\mu}|p_1, p_2\rangle_{\text{in}}. \quad (5.7)$$

From now on we will drop the breve and infer from the arguments the type of f we are dealing with. The KMOC framework concerns itself with the change of an observable during a scattering event. For such an observable O, its change can be simply obtained by evaluating the difference of the expectation value of the corresponding Hermitian operator, $\mathbb{O}$, between in and out states

$$\Delta O = \langle\text{out}|\mathbb{O}|\text{out}\rangle - \langle\text{in}|\mathbb{O}|\text{in}\rangle.$$

In quantum mechanics, the out states are related to the in states by the time evolution operator, i.e. the S-matrix: $|\text{out}\rangle = S|\text{in}\rangle$ and we can write

$$
\begin{aligned}
\Delta O &= \langle\text{in}|S^\dagger\mathbb{O}S|\text{in}\rangle - \langle\text{in}|\mathbb{O}|\text{in}\rangle \\
&\overset{S^\dagger S = \mathbb{1}}{=} \langle\text{in}|S^\dagger[\mathbb{O}, S]|\text{in}\rangle \\
&\overset{S = \mathbb{1} + iT}{=} \langle\text{in}|[\mathbb{O}, \mathbb{1} + iT]|\text{in}\rangle - \langle\text{in}|iT^\dagger[\mathbb{O}, \mathbb{1} + iT]|\text{in}\rangle \quad (5.8)\\
&= \langle\text{in}|i[\mathbb{O}, T]|\text{in}\rangle + \langle\text{in}|T^\dagger[\mathbb{O}, T]|\text{in}\rangle \\
&= \Delta O_{\text{v}} + \Delta O_{\text{r}}.
\end{aligned}
$$

In order, we use the unitarity of the S-matrix, then express the S-matrex as the identity (no actual interaction) and the transfer matrix T. The commutators are then expanded and the part with the identity vanish (as $\mathbb{1}$ commutes with everything).

If we put in the definition of our in state (5.7) we have:

$$\Delta O = \int d\Phi_4(p_1, p_2, p_1', p_2')\, f_1(p_1)f_2(p_2)f^*{}_1(p_1')f^*{}_2(p_2')\, e^{ib_\mu \frac{p_1{}^\mu - p_1'{}^\mu}{\hbar}}\left[\mathcal{I}_{\text{v}}(O) - \mathcal{I}_{\text{r}}(O)\right].$$

Where we define the real integrand $\mathcal{I}_{\text{r}}(O)$ and the virtual integrand $\mathcal{I}_{\text{v}}(O)$ as the following matrix elements:

$$
\begin{aligned}
\mathcal{I}_{\text{v}}(O) &= {}_{\text{in}}\langle p_1' p_2'|i[\mathbb{O}, T]|p_1 p_2\rangle_{\text{in}} \\
\mathcal{I}_{\text{r}}(O) &= {}_{\text{in}}\langle p_1' p_2'|T^\dagger[\mathbb{O}, T]|p_1 p_2\rangle_{\text{in}}.
\end{aligned}
$$

Let us first look at the virtual integrand $\mathcal{I}_{\text{v}}(O)$:[44]

[44] Here we define
$$O_{\text{in}}|p_1 p_2\rangle = \mathbb{O}|p_1 p_2\rangle$$

aswell as,

$$O'_{\text{in}}\langle p_1' p_2'| = \langle p_1' p_2'|\mathbb{O}$$

and finally

$$\underset{p'-p}{\Delta}O = O'_{\text{in}} - O_{\text{in}}$$

NB: the notation is slightly different in the **Bern:2021xze** paper

$$\mathcal{I}_{\mathrm{v}}(O) = {}_{\mathrm{in}}\langle p_1' p_2' | \mathring{i}[\mathbb{O}, T] | p_1 p_2\rangle_{\mathrm{in}}$$
$$= {}_{\mathrm{in}}\langle p_1' p_2' | \mathring{i}\mathbb{O}T | p_1 p_2\rangle_{\mathrm{in}} - {}_{\mathrm{in}}\langle p_1' p_2' | \mathring{i}T\mathbb{O} | p_1 p_2\rangle_{\mathrm{in}}$$
$$= \mathring{i}O_{\mathrm{in}'} \, {}_{\mathrm{in}}\langle p_1' p_2' | T | p_1 p_2\rangle_{\mathrm{in}} - \mathring{i}O_{\mathrm{in}} \, {}_{\mathrm{in}}\langle p_1' p_2' | T | p_1 p_2\rangle_{\mathrm{in}}$$
$$= \mathring{i}\Delta O_{p'-p} \, {}_{\mathrm{in}}\langle p_1' p_2' | T | p_1 p_2\rangle_{\mathrm{in}}$$
$$= \mathring{i}\Delta O_{p'-p} \, \tilde{\delta}^4(p_1 + p_2 - p_1' - p_2') \mathcal{A}(p_1, p_2 \to p_1', p_2').$$

Note that the amplitude is from in states to in states! Now for the real integrand $\mathcal{I}_{\mathrm{r}}(O)$ we insert a complete set of states :[45]

$$\mathcal{I}_{\mathrm{r}}(O) = {}_{\mathrm{in}}\langle p_1' p_2' | T^\dagger[\mathbb{O}, T] | p_1 p_2\rangle_{\mathrm{in}}$$
$$= \sum_X \int \mathrm{d}\Phi_{2+|X|}(r_1, r_2, X) \, {}_{\mathrm{in}}\langle p_1' p_2' | T^\dagger | r_1 r_2 X\rangle\langle r_1 r_2 X | [\mathbb{O}, T] | p_1 p_2\rangle_{\mathrm{in}}$$
$$= \sum_X \int \mathrm{d}\Phi_{2+|X|}(r_1, r_2, X) \, \tilde{\delta}^4(p_1 + p_2 - r_1 - r_2 - r_X) \, \mathcal{A}(p_1, p_2 \to r_1, r_2, r_X)$$
$$\Delta O_{rX-p} \, \tilde{\delta}^4(p_1' + p_2' - r_1 - r_2 - r_X) \, \mathcal{A}^*(p_1', p_2' \to r_1, r_2, r_X).$$

For both integrands we can preform some variable changes and eliminate certain delta functions. We introduce momentum shifts $q_i = p_i' - p_i$ and then integrate over q_2 finally relabelling $q_1 \to q$ [46]. Thus we have

$$\Delta O_{\mathrm{v}} = \int \mathrm{d}\Phi_2(p_1, p_2) \, \tilde{\mathrm{d}}^4 q \, \tilde{\delta}(2p_1 \cdot q + q^2)\Theta(p_1^0 + q^0) \, \tilde{\delta}(2p_2 \cdot q - q^2)\Theta(p_2^0 - q^0)$$
$$\times f_1(p_1) f_2(p_2) f^*_1(p_1 + q) f^*_2(p_2 - q) \, e^{-\frac{i}{\hbar} b_\mu q^\mu}$$
$$\times \mathring{i}\Delta O_q \, \mathcal{A}(p_1, p_2 \to p_1 + q, p_2 - q), \tag{5.9}$$

$$\Delta O_{\mathrm{r}} = \sum_X \int \mathrm{d}\Phi_{2+|X|}(r_1, r_2, X) \, \mathrm{d}\Phi_2(p_1, p_2) \, \tilde{\mathrm{d}}^4 q \, \tilde{\delta}(2p_1 \cdot q + q^2)\Theta(p_1^0 + q^0)$$
$$\times \tilde{\delta}(2p_2 \cdot q - q^2)\Theta(p_2^0 - q^0)$$
$$\times f_1(p_1) f_2(p_2) f^*_1(p_1 + q) f^*_2(p_2 - q) \, e^{-\frac{i}{\hbar} b_\mu q^\mu}$$
$$\times \Delta O_{rX-p} \, \tilde{\delta}^{(4)}(p_1 + p_2 - r_1 - r_2 - r_X) \, \tilde{\delta}^{(4)}$$
$$\times \mathcal{A}(p_1, p_2 \to r_1, r_2, r_X)\mathcal{A}^*(p_1 + q, p_2 - q \to r_1, r_2, r_X). \tag{5.10}$$

We have arrived at an integral expression for the change in observable O. Luckily for us, we will not need to perform these integrals in the classical limit. We will just have carefully chosen replacement rules for the integrated variables! Let us look at this in more detail now.

5.3.1 Classical limit

Since we are concerned with classial observables we need to explore the classical limit of 5.8, i.e. the limit of $\hbar \to 0$. The first target is the wavefunctions.

5.3.1.1 Classical limit of wavefunctions

In KMOC framework we are interested in the classical limit of a scattering event. It is then important to understand the precise simplifications this limit yields.

We have multiple conditions on the wavefunctions. The first are those imposed by LSZ reduction. That is,

- Compact support momentum space wavefunction
- Peaked around one value of momenta

Classical limit of the wavefunctions should make sense, thus

1. as $\hbar \to 0$ the position and momentum wavefunction should approach delta functions, centered around their classical values.
2. The overlap between the wavefunction and its conjugate should be nearly full, since they represent the same particle classically.

Consider for example a nonrelativistic wavefunction for a particle of mass m:

$$f(\mathbf{p}) = \exp\left(-\frac{\mathbf{p}}{2\hbar m \ell_c / \ell_\omega^2}\right) \stackrel{\hbar = \ell_c m}{=} \exp\left(-\frac{\mathbf{p}}{2m^2 \ell_c^2 / \ell_\omega^2}\right),$$

where ℓ_c is the compton wavelength of the particle $\frac{\hbar}{m}$ and ℓ_ω is a characteristic width. This wavefunction grows sharper in

the $\hbar \to 0$ limit. If we now take the Fourier transform of $f(\mathbf{p})$ to gives us the position "probability density", we have:[47]

$$\mathcal{F}_{\mathbf{p}}^{-1}[f](\mathbf{x}) = \int \frac{\mathrm{d}\mathbf{p}}{2\pi} \exp\left(-(\frac{\mathbf{p}}{A})^2\right) \exp\left(-\frac{\mathring{i}}{\hbar}\mathbf{p}\cdot\mathbf{x}\right)$$

$$= \frac{1}{2\pi} \underbrace{\int \mathrm{d}\mathbf{p} \, \exp\left(-\left(\frac{\mathbf{p}}{A} - \frac{\mathring{i}\mathbf{x}A}{2\hbar}\right)^2\right)}_{\sqrt{\pi}A} \exp\left(-\frac{\mathbf{x}^2 A}{4\hbar^2}\right)$$

$$= \frac{\sqrt{2}A}{2\pi} \exp\left(-\frac{\mathbf{x}^2}{2\ell_\omega^2}\right).$$

This elucidates more clearly the meaning of characterisic width, as ℓ_ω is the width of the wavefunction in position space. Thus, the position space-wavefunction grows sharper in the $\ell_\omega^2 \to 0$ limit. For both wavefunctions to simultaneously grow sharper in the classical limit, we must then have that $\xi = (\frac{\ell_c}{\ell_\omega})^2 \to 0$ remembering that the $\hbar \to 0$ limit is just given by the $\ell_c \to 0$ one. Finally the meaning of classical limit in this context is the $\xi \to 0$ limit.

Going back to the general conditions we want a wavefunction $f_i(p_i)$ s.t in the classical limit the momentum reaches it's classical value: $\breve{p}_i = m_i\breve{u}_i$, with $\breve{u}_i$ the classical four-velocity of particle i, normalized to $\breve{u}_i^2 = 1$.

$$\langle p_i{}^\mu \rangle = \int \mathrm{d}\Phi(p_i)\, p_i{}^\mu |f_i(p_i)|^2 \overset{!}{=} m_i\breve{u}_i^\mu(1 + \mathcal{O}(\xi^{\beta'}))$$

where β' encodes the speed at which the classical value is reached in the $\xi \to 0$ limit. The velocity normalization convergence is controlled by β'':

$$\breve{u}_i \cdot u_i = 1 + \mathcal{O}(\xi^{\beta''})$$

And finally wavefunction spread is controlled by β, and must converge to 0:

$$\sigma^2(p_i)/m_i^2 = \frac{1}{m_i^2}\langle (p_i - \langle p_i \rangle)^2 \rangle$$

$$= \frac{1}{m_i^2}(\langle p_i^2 \rangle - \langle p_i \rangle^2)$$

$$= \frac{1}{m_i^2}(m_i^2 - (m_i\breve{u}_i(1 + \mathcal{O}(\xi^{\beta'})))^2)$$

$$\propto \xi^\beta,$$

where $\langle p_i^2 \rangle = m_i^2$ is enforced by the measure $\mathrm{d}\Phi(p)$.

Additionally the wavefunction should be Lorentz invariant, thus naively we would have that $f(p_i^\mu) = f'(p_i^2)$. However the integration measure enforces an on-shell condition: $m_i^2 = p_i^2$. Thus the wavefunction cannot usefully depend on p_i^2, and we need to introduce at least one additional four vector parameter u. The simplest dimensionless combination of parameters it then $\frac{p \cdot u}{m}$. Of course the wavefunction must also depend on ξ and the simplest form of argument will thus be $\frac{p \cdot u}{m\xi}$ so that any p not aligned with u will be strongly suppressed in the $\xi \to 0$ limit.

We now have control over most of the conditions:

- The classical limit is well defined
- The wavefunction spread is controlled
- The arguments of the wavefunction are clear

We can write a general wavefunction that satisfies the above as:

$$f(\frac{p \cdot u}{m} | \breve{u}_i; m_i; \beta^{(i)}).$$

This function can take the form of a gaussian, or something similar to 5.5. Now there is one final requirement, that concerns the overlap of f and f^* must be $\mathcal{O}(1)$, equivalently and more precisely:

$$f^*(p+q) \sim f^*(p) \implies f^*(p+q) - f^*(p) \ll 1 \implies q^\mu \frac{\partial}{\partial p^\mu} f^*(p) \ll 1.$$

Making explicit the $\frac{p \cdot u}{m\xi}$ dependence: $f(p) = \varphi(\frac{p \cdot u}{m\xi})$ for $\varphi(x)$ a scalar function.

$$\implies \frac{q^\mu u_\mu}{m\xi} \frac{\mathrm{d}\varphi^*(x)}{\mathrm{d}x}\bigg|_{\frac{p \cdot u}{m\xi}} \ll 1.$$

Thus we require that for a characteristic value of $q = q_0$ we have:

$$\frac{q_0 \cdot u}{m\xi} = \bar{q}_0 \cdot u \frac{\ell_\omega^2}{\ell_c} \ll 1 \iff \bar{q}_0 \cdot u \, \ell_\omega \ll \sqrt{\xi},$$

where we denote by a bar, any quantity that has been rescaled by $\hbar$. Thus a momentum p when divided by $\hbar$ will be written $\bar{p}$ and called wavenumber. We will combine this inequality with ones we obtain from the specific cases of integrations required above.

We now want to examine the classical limit of something like 5.9. If we consider just the integration over the initial momenta p_i and the initial wavefunctions with $\tilde{\delta}(2p_i \cdot q + q^2)$, the delta function will smear out to a sharply peaked function whose scale is the same order as the original wavefunctions. As ξ gets smaller, this function will turn back into a delta function imposed on the q integration. Let us examine this statement more closely. We are interested in the classical limit of the integrals such as:

$$d(m, \xi, u, q) = \int \mathrm{d}\Phi(p)\, \tilde{\delta}(2p \cdot q + q^2)\Theta(p^0 + q^0)\varphi(\frac{p \cdot u}{m\xi})\varphi^*(\frac{(p+q) \cdot u}{m\xi}).$$
$$(5.11)$$

This integral must be Lorentz invariant and depends on m, ξ, u, q thus it must manifestly only depend on the following Lorentz invariants: $u^2, q^2, u \cdot q, \xi$. One of these is not actually a variable as we will normalise $u^2 = 1$. The rest aren't fully dimensionless, and we can render them dimensionless:

$$[q^2] = [\hbar\bar{q}]^2 = [M]^2 \implies [\ell_c\sqrt{-\bar{q}^2}] = [\frac{\hbar}{m}\sqrt{-\bar{q}^2}] = \frac{[M]}{[M]} = 1,$$

$$[u \cdot q] = [M] \implies [\frac{u \cdot \bar{q}}{\sqrt{-\bar{q}^2}}] = [\frac{u \cdot q}{\sqrt{-q^2}}] = \frac{[M]}{[M]} = 1,$$

$$[\xi] = 1.$$

If we call $\frac{1}{\sqrt{-\bar{q}^2}} = \ell_s$ a scattering length[48] then our dimensionless ratios become :

[48] t $[\frac{1}{\sqrt{-\bar{q}^2}}] = [T] = [L] = [\ell_s]$

$$\frac{\ell_c}{\ell_s} \quad \text{and} \quad \ell_s\, \bar{q} \cdot u.$$

The delta function can then be rewritten as:

$$\tilde{\delta}(2p \cdot q + q^2) = \tilde{\delta}(2\hbar m\, u \cdot \bar{q} + \hbar^2 \bar{q}^2) = \frac{1}{\hbar m}\tilde{\delta}(2\bar{q} \cdot u - \frac{\ell_c}{\ell_s^2}) = \frac{\ell_s}{\hbar m}\tilde{\delta}(2\ell_s\, \bar{q} \cdot u - \frac{\ell_c}{\ell_s}).$$

Performing the integration over p in 5.11 we obtain symbolically:

$$d(m, \xi, u, q) = \text{peaked function imposing that } 2\ell_s\, \bar{q} \cdot u = \frac{\ell_c}{\ell_s} \text{ with width } \xi^\beta.$$

```julia
using Plots

function delta(x)
    if abs(x)<1e-3
        return 1
    else
        return 0
    end
end

function gauss(x)
    return exp(-x^2)
end

function sharpen(f,eps,power)
    return x->f(x/eps^power)/eps^power
end

epss=0.02:0.01:0.1


p=plot([sharpen(gauss,eps,1) for eps in epss], -0.5,0.5,label=epss')
```
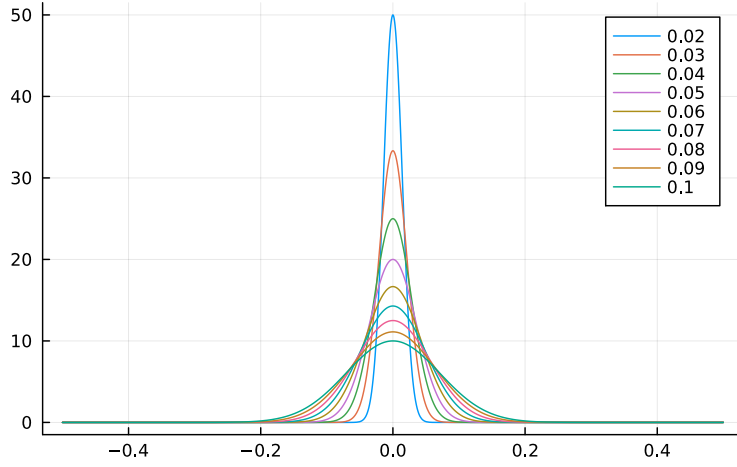
Let us disucss the wavefunction and the scales a bit more physically. The characteristic width ℓ_ω is the particle's position uncertainty, $\frac{\hbar}{\ell_\omega}$ is the associated momentum uncertainty. In the classical limit it makes sense that the position uncertainty is neglible with respect to minimum distance between the particles ℓ_s:

$$\ell_\omega \ll \ell_s,$$

and the momentum uncertainty is neglible with respect to the masses of the particles:

$$\frac{\hbar}{\ell_\omega} \ll m \implies \ell_c \ll \ell_\omega.$$

Putting these together we obtain the goldilocks inequality:

$$\ell_c \ll \ell_\omega \ll \ell_s.$$

Now we can go back and look at the arguments of d and we see that

$$\ell_s \, \bar{q} \cdot u \gg \ell_\omega \bar{q} \cdot u \sim \sqrt{\xi} = \frac{\ell_c}{\ell_\omega} \gg \frac{\ell_c}{\ell_s}.$$

Thus in the classical limit we have that d collapses to:

61

$$d(m, \xi, u, q) \propto \tilde{\delta}(\bar{q} \cdot u).$$

Thus the wavefunction-weighted on-shell phase-space integration disappears in the classical limit! The only condition is that the integration momenta take on their physical values. The sequence that we have gone through should be done for all the integrands of type d. We will not do this explicitly every time but instead apply the following rules:

1. Just as for the massless transfer momentum any messenger momentum, be it transfer, virtual-loop or real emmission, shall become a wavenumber: $k \to \hbar \bar{k}$.
2. Replace all couplings with their dimensionless counterparts: $\kappa \to \frac{\kappa}{\sqrt{\hbar}}$ (this is only precisely true for SQED and gravity, which are the applications we are interested in).
3. Eliminate all on-shell integrations by approximating $f(p + \hbar \bar{q})$ by $f(p)$.
4. Laurent expand all the integrands in $\hbar$.
5. Make the integration momenta take on their physical values: $p_i \to m_i \breve{u}_i$.

To make this idea explicit we introduce the following notation, meaning that the steps above have been applied:

$$\left\langle\!\!\left\langle\!\!\left\langle g(p_1, p_2, \dots) \right\rangle\!\!\right\rangle\!\!\right\rangle \overset{\text{def}}{=} \int d\Phi(p_1) \, d\Phi(p_2) \, |f_1(p_1)|^2 |f_2(p_2)|^2 \, g(p_1, p_2, \dots)$$

We can now rewrite 5.8:

$$\Delta O = \left\langle\!\!\left\langle\!\!\left\langle \int \overbrace{\tilde{d}^4 q \, \tilde{\delta}(2p_1 \cdot q + q^2) \Theta(p_1{}^0 + q^0) \tilde{\delta}(2p_2 \cdot q - q^2) \Theta(p_2{}^0 + q^0)}^{d\Psi(q)} e^{-\frac{i}{\hbar} q^\mu b_\mu} \left(\mathcal{J}'_{\text{v}}(O) + \mathcal{J}'_{\text{r}}(O) \right) \right\rangle\!\!\right\rangle\!\!\right\rangle,$$

$$(5.12)$$

where

$$\mathcal{J}'_{\text{v}}(O) = i \underset{q}{\Delta O} \, \mathcal{A}(p_1, p_2 \to p_1 + q, p_2 - q)$$

$$\mathcal{J}'_{\text{r}}(O) = \sum_X \int d\Phi_{2+|X|}(r_1, r_2, X) \underset{rX-p}{\Delta O} \, \tilde{\delta}^{(4)}(p_1 + p_2 - r_1 - r_2 - r_X)$$

$$\times \, \mathcal{A}(p_1, p_2 \to r_1, r_2, r_X) \mathcal{A}^*(p_1 + q, p_2 - q \to r_1, r_2, r_X).$$

Additionally we want to make clear the dependence on $\hbar$ since we want to eventually take the $\hbar \to 0$ limit. We apply step 1. above, and change integration variables to $\bar{q} = \frac{q}{\hbar}$ and absorb that $\hbar$ dependence into the redefinition of the integrands and the measure:

$$\mathrm{d}\Psi(q) = \hbar^2 \, \mathrm{d}\overline{\Psi}(\bar{q}) = \hbar^4 \, \tilde{\mathrm{d}}^4\bar{q} \, \frac{1}{\hbar}\tilde{\delta}(2p_1 \cdot \bar{q} + \hbar\bar{q}^2)\Theta(p_1{}^0 + q^0)\frac{1}{\hbar}\tilde{\delta}(2p_1 \cdot \bar{q} + \hbar\bar{q}^2)\Theta(p_2{}^0 + q^0),$$

$$\overline{\mathcal{J}'_{\mathrm{v}}}(O) = \hbar^2 \mathcal{J}'_{\mathrm{v}}(O),$$
$$\overline{\mathcal{J}'_{\mathrm{r}}}(O) = \hbar^2 \mathcal{J}'_{\mathrm{r}}(O).$$

We can finally neatly write:

$$\Delta O = \left\langle\!\!\left\langle \int \mathrm{d}\overline{\Psi}(\bar{q}) \, \mathrm{e}^{-i\bar{q}^\mu b_\mu} \left(\overline{\mathcal{J}'_{\mathrm{v}}}(O) + \overline{\mathcal{J}'_{\mathrm{r}}}(O) \right) \right\rangle\!\!\right\rangle.$$

Now the $\hbar$ dependence is all in the integrands (ignoring the $\hbar\bar{q}^2$ factors in the delta function). The classical limit of this observable is then simply, dropping the angle brackets, since these dissappear in the classical limit:

$$\Delta O_{\mathrm{classical}} = \lim_{\hbar \to 0} \hbar^{\beta_{LO}} \left[\int \mathrm{d}\overline{\Psi}(\bar{q}) \left(\overline{\mathcal{J}'_{\mathrm{v}}}(O) + \overline{\mathcal{J}'_{\mathrm{r}}}(O) \right) \right],$$

where β_{LO} is the LO $\hbar$-dependence of the observable. This is so that $\Delta O_{\mathrm{classical}} \sim \hbar^0$ i.e. classical scaling.

5.4 Impulse in KMOC

We can now explore the integrands for a specific observable. Consider the momentum of particle 1, $p_1{}^\mu$, then the change in momentum is essentially the impulse of particle 1. The KMOC formalisms gives us a way to write this as:

$$\Delta p_1{}^\mu = \left\langle\!\!\left\langle \int \mathrm{d}\overline{\Psi}(\bar{q}) \, \exp\left(-i\bar{q}^\mu b_\mu \right) \left(\overline{\mathcal{J}'_{\mathrm{v}}}(p_1{}^\mu) + \overline{\mathcal{J}'_{\mathrm{r}}}(p_1{}^\mu) \right) \right\rangle\!\!\right\rangle.$$

We then have:

$$\overline{\mathcal{J}'_{\mathrm{v}}}(p_1{}^\mu) = \hbar^2 \mathring{i}\, q\, \mathcal{A}(p_1, p_2 \to p_1 + \hbar\bar{q}, p_2 - \hbar\bar{q})$$

$$\overline{\mathcal{J}'_{\mathrm{r}}}(p_1{}^\mu) = \hbar^2 \; \mathrm{d}\Phi_{2+|X|}(r_1, r_2, r_X)\, (r_1^\mu - p_1^\mu)\, \tilde{\delta}^{(4)}(p_1 + p_2 - r_1 - r_2 - r_X)$$

$$\times\, \mathcal{A}(p_1, p_2 \to r_1, r_2, r_X) \mathcal{A}^*(p_1 + \hbar\bar{q}, p_2 - \hbar\bar{q} \to r_1, r_2, r_X).$$

We can extract $\hbar$ from q and from the amplitude, by extracting each coupling constant κ along with an $\frac{1}{\sqrt{\hbar}}$, thus quartic vertices yield a factor of $\frac{\kappa^2}{\hbar}$ whereas cubic ones yield $\frac{\kappa}{\sqrt{\hbar}}$[49]. If we count the number V_3 of all cubic vertices, V_4 the number of quartic vertices, and so on, we have that the number of internal lines is $I = \frac{1}{2}(\sum_{d=3} dV_d - E)$. This is because we have $\sum_{d=3} dV_d$ lines to start with, out of which E are chosen to be external. The remaining $(\sum_{d=3} dV_d - E)$ ones are contracted among themselves to form I internal lines. In our case we have $E = 4 + M$ where $M = |X|$ is the number of messenger particles. Using the argument from loop counting we have that the number of loops of our graph L is given by:

$$L = I - V + N = \frac{1}{2}\left(\sum_{d=3} d \cdot V_d - 4 - M\right) - \sum_{d=3} V_d + 1$$

$$= \frac{1}{2}\left(\sum_{d=3}(d-2)V_d\right) - 1 - \frac{M}{2},$$

where N is the number of connected components ($= 1$ in our case) . Thus we see that the amount of extracted $\hbar$s corresponds directly to the number of loops plus one[50]! We can thus write the amplitude $\mathcal{A}$ as a sum over reduced L-loop amplitudes $\bar{\mathcal{A}}^{(L)}$:

$$\mathcal{A}(p_1, p_2 \to r_1, r_2, X) = \sum_{L=0}^{\infty} \left(\frac{\kappa^2}{\hbar}\right)^{(L+1+\frac{|X|}{2})} \bar{\mathcal{A}}^{(L)}(p_1, p_2 \to r_1, r_2, X).$$

Going back to the integrands we have:

$$\overline{\mathcal{J}'_{\mathrm{v}}}(p_1{}^\mu) = \hbar^3 \mathring{i}\, \bar{q} \sum_{L=0}^{\infty} \left(\frac{\kappa^2}{\hbar}\right)^{(L+1)} \bar{\mathcal{A}}^{(L)}(p_1, p_2 \to p_1 + \hbar\bar{q}, p_2 - \hbar\bar{q})$$

$$= \mathring{i}\, \hbar\bar{q} \sum_{L=0}^{\infty} \kappa^{2(L+1)} \hbar^{(1-L)} \bar{\mathcal{A}}^{(L)}(p_1, p_2 \to p_1 + \hbar\bar{q}, p_2 - \hbar\bar{q}),$$

$$(5.13)$$

[49] as mentioned in the last section, this is true for gravity and SQED and we will extend this fact to schematically rescale the vertex coupling by $\hbar^{-\frac{d-2}{2}}$, for d the degree of the vertex in question.

[50] and the number of extracted couplings being twice that

as well as the real kernel:[51]

$$\overline{\mathcal{J}'_r}(p_1{}^\mu) = \hbar^2 \, d\Phi_{|X|}(r_X) \Big[\prod_{i=1,2} \tilde{d}^4 w_i \, \tilde{\delta}(2p_i \cdot w_i + w_i^2) \Theta(p_i^0 + w_i^0) \Big]$$
$$\times \, w_1^\mu \, \tilde{\delta}^{(4)}(w_1 + w_2 + r_X)$$
$$\times \, \mathcal{A}(p_1, p_2 \to p_1 + w_1, p_2 + w_2, r_X) \mathcal{A}^*(p_1 + \hbar\bar{q}, p_2 - \hbar\bar{q} \to p_1 + w_1, p_2 + w_2, r_X)$$

$$= \hbar^2 \, d\Phi_{|X|}(r_X) \Big[\prod_{i=1,2} \hbar^3 \, \tilde{d}^4 \bar{w}_i \, \tilde{\delta}(2p_i \cdot \bar{w}_i + \hbar\bar{w}_i^2) \Theta(p_i^0 + \hbar\bar{w}_i^0) \Big]$$
$$\times \, \hbar\bar{w}_1^\mu \, \hbar^{-4} \tilde{\delta}^{(4)}(\bar{w}_1 + \bar{w}_2 + \bar{r}_X)$$
$$\times \sum_{L=0}^{\infty} \left(\frac{\kappa^2}{\hbar} \right)^{(2L+2+|X|)} \bar{\mathcal{A}}^{(L)}(p_1, p_2 \to p_1 + \hbar\bar{w}_1, p_2 + \hbar\bar{w}_2, r_X)$$
$$\times \, \bar{\mathcal{A}}^{*(L)}(p_1 + \hbar\bar{q}, p_2 - \hbar\bar{q} \to p_1 + \hbar\bar{w}_1, p_2 + \hbar\bar{w}_2, r_X)$$

$$= \, d\Phi_{|X|}(r_X) \Big[\prod_{i=1,2} \tilde{d}^4 \bar{w}_i \, \tilde{\delta}(2p_i \cdot \bar{w}_i + \hbar\bar{w}_i^2) \Theta(p_i^0 + \hbar\bar{w}_i^0) \Big]$$
$$\times \, \hbar\bar{w}_1^\mu \, \tilde{\delta}^{(4)}(\bar{w}_1 + \bar{w}_2 + \bar{r}_X)$$
$$\times \sum_{L=0}^{\infty} \kappa^{2(2L+2+|X|)} \hbar^{2-2L-|X|} \bar{\mathcal{A}}^{(L)}(p_1, p_2 \to p_1 + \hbar\bar{w}_1, p_2 + \hbar\bar{w}_2, r_X)$$
$$\times \, \bar{\mathcal{A}}^{*(L)}(p_1 + \hbar\bar{q}, p_2 - \hbar\bar{q} \to p_1 + \hbar\bar{w}_1, p_2 + \hbar\bar{w}_2, r_X). \tag{5.14}$$

Schematically we have

$$\overline{\mathcal{J}'_v}(p_1{}^\mu) = \sum_{L=0}^{\infty} \mathcal{O}(\kappa^{2(L+1)}),$$
$$\overline{\mathcal{J}'_r}(p_1{}^\mu) = \sum_{L=0}^{\infty} \mathcal{O}(\kappa^{4(L+1)+2|X|})$$

The contributions from the virtual kernel are lower order in the coupling κ for a given loop order. Both kernels contribute together provided that the following equation is verified:

$$L - 1 = 2L' + |X|. \tag{5.15}$$

Where L is the loop count for the virtual kernel and L', $|X|$ are the real kernel loop count and messenger particle count

respectively. Note that for a tree level virtual kernel, the real-kernel match does not exist. The real kernel is only present for $L > 0$. When taking the classical limit we will only retain contributions from graphs that cancel the $\hbar$ divergences in each corresponding kernel. Thus at L loop level, the amplitude in the virtual kernel must cancel with:

$$\hbar^{1-L+O}, \tag{5.16}$$

where the O term is the order of $\hbar$ that is present as a result of the observable. In the case of particle 1's momentum, $O = 1$. Similarly, the amplitudes in the real kernel must cancel with:

$$\hbar^{2-2L-|X|+O'}. \tag{5.17}$$

Now we see that the LO contribution [52] to the impulse $\Delta p_1^{\mu,(0)}$ can only be from the virtual kernel at tree level. Thus we have the following equation,

$$\Delta p_1^{\mu,(0)} = \left\langle\!\!\!\left\langle \int d\overline{\Psi}(\bar{q}) \, \exp\left(-i\mathring{\bar{q}}^{\mu} b_{\mu}\right) \, \overline{\mathcal{J}_{\mathrm{v}}'}(p_1^{\mu})^{(L=0)} \right\rangle\!\!\!\right\rangle. \tag{5.18}$$

And the integrand is given by the tree level 4 point amplitude.

$$\overline{\mathcal{J}_{\mathrm{v}}'}(p_1^{\mu})^{L=0} = \mathring{i} \, \bar{q}^{\mu} \, \kappa^2 \hbar^2 \bar{\mathcal{A}}^{(0)}(p_1, p_2 \to p_1 + \hbar\bar{q}, p_2 - \hbar\bar{q}).$$

At Next-to-Leading Order (), i.e. κ^4 order, both integrands contribute, as 5.15 can be satisfied for $L = 1$, $L' = 0$ and $|X| = 2$. Thus we have the following equation:

$$\Delta p_1^{\mu,(1)} = \left\langle\!\!\!\left\langle \int d\overline{\Psi}(\bar{q}) \, \exp\left(-i\mathring{\bar{q}}^{\mu} b_{\mu}\right)\left(\overline{\mathcal{J}_{\mathrm{v}}'}(p_1^{\mu})^{(L=1)} + \overline{\mathcal{J}_{\mathrm{r}}'}(p_1^{\mu})^{(L'=0)}\right) \right\rangle\!\!\!\right\rangle. \tag{5.19}$$

The virtual integrand is now given by the 1-loop level amplitude, and the real integrand is given by the square of a the

[52] Here the expansion is in powers of the coupling constant, so even though we want $\hbar$s to cancel, the loop order will still affect the order of the contribution through the coupling constant κ and the LO corresponds to κ

tree level amplitude. This process can go on indefinetely, and is general to the the type of observable and the theory. Here we considered the change of momentum a particle, which for a black hole very far away would be very difficult to measure. However, we can also consider an observable such as the four-momentum of the radiated particles, or more precisely its expection value. Of course the operator corresponding to this observable gives zero when acting on the initial momentum states, and only gives a non-zero result when acting on the messenger states. Thus for this observable only the real integrand, starting with $|X| = 1$ will contribute, the LO contrybution being given by what is essentially the unitarity cut of a two loop amplitude. We see that regardless of observable, the objects that are needed are the amplitudes.

For each loop level, many diagrams can contribute, but the classical limit enforces that they must cancel the $\hbar$ orders given by 5.17 and 5.16. The cancellation order is dependent on the considered observable and filters the contributing diagrams. It can also be reformulated in the language of the method of regions.

To see the whole machinery in action, let us take SQED as an example theory, that shows the relevant subleties of the formalism.

5.5 SQED amplitudes

We want to couple a set of massive scalar fields to electromagnetism. We will use the minimal coupling prescirption to ensure that the resulting lagrangian exhibits the required gauge symmetry. The minimal coupling prescription works provided that our base mass lagrangian admits a conserved current. Our base mass lagrangian for two complex scalar fields is:

$$\mathcal{L}_m = \sum_{i=1}^{2} \partial_\mu \phi_i^\dagger \, \partial^\mu \phi_i - m_i^2 \phi_i^\dagger \phi_i.$$

Notice that under the following transformation:

$$\phi_i(x) \rightarrow e^{-iQ_i\lambda}\phi_i(x),$$
$$\phi_i^\dagger(x) \rightarrow e^{iQ_i\lambda}\phi_i^\dagger(x),$$

or infinitesimally:

$$\delta\phi_i = -i\phi_i Q_i \delta\lambda,$$
$$\delta\phi_i^\dagger = i\phi_i^\dagger Q_i \delta\lambda,$$

the above Lagrangian is unchanged. We will identitfy Q_i with the charge, in units of e, of each particle. Note the sign of the transformation is important. If we upgrade the parameter λ to a spacetime function $\lambda(x)$, the Lagrangian is not invariant anymore and invariance is restored if we replace all the derivatives ∂_μ with the gauge-covariant derivative D_μ, i.e. if along with the transformation above, we perform a gauge transformation of the photon field:

$$A_\mu \rightarrow A_\mu + \frac{1}{e}\partial_\mu\lambda$$

or infinitesimally

$$\delta A_\mu = \frac{1}{e}\partial_\mu\delta\lambda,$$

then the whole lagrangian:

$$\mathcal{L}_{ED} + \mathcal{L}_m(\phi_i, \partial_\mu\phi_i) \rightarrow \mathcal{L}_{ED} + \mathcal{L}_m(\phi_i, D_\mu\phi_i),$$

is invariant under the above defined gauge transformation, with the gauge-covariant derivative defined as:

$$D_\mu = \partial_\mu + i\,e\,Q_i\,A_\mu.$$

The final lagrangian is:

$$\mathcal{L} = -\frac{1}{4}F_{\mu\nu}F^{\mu\nu} + \sum_{i=1}^{2}\left[(D_\mu\phi_i)^\dagger (D^\mu\phi_i) - m_i^2\phi_i^\dagger\phi_i\right],$$

with $F_{\mu\nu} \equiv \partial_\mu A_\nu - \partial_\nu A_\mu$. Expanding and then integrating
by parts:

$$\mathcal{L} = -\frac{1}{4}\left(\partial_\mu A_\nu - \partial_\nu A_\mu\right)\left(\partial^\mu A^\nu - \partial^\nu A^\mu\right) + \sum_{i=1}^{2}\left[\left(\partial_\mu - i\,e\,Q_i\,A_\mu\right)\phi_i^\dagger\left(\partial_\mu + i\,e\,Q_i\,A_\mu\right)\phi_i - m_i^2\phi_i^\dagger\phi_i\right]$$

$$= \underbrace{\frac{1}{2}A_\mu\left[\eta^{\mu\nu}\partial^2 - \partial^\mu\partial^\nu\right]A_\nu + \sum_{i=1}^{2}-\phi_i^\dagger\left(\partial^2 + m_i^2\right)\phi_i}_{\mathcal{L}_0} + \underbrace{\sum_{i=1}^{2}q_i^2\,e^2 A_\mu A^\mu\,\phi_i^\dagger\phi_i - i\,e\,Q_i\,A_\mu\left(\phi_i^\dagger\partial^\mu\phi_i - \left(\partial^\mu\phi_i^\dagger\right)\phi_i\right)}_{\mathcal{L}'}.$$

Since we have a massless photon, and still have gauge freedom
we have to implement gauge fixing in the usual way:

$$\mathcal{L}_{\text{eff}} = \mathcal{L} + \overbrace{\frac{-1}{2\xi}\left(\partial_\mu A^\mu\right)^2}^{\mathcal{L}_{\text{GF}}}$$

$$= \frac{1}{2}A_\mu \underbrace{\left[g^{\mu\nu}\partial^2 - \left(1 - \frac{1}{\xi}\right)\partial^\mu\partial^\nu\right]}_{\rightarrow \tilde{D}_\xi^{\mu\nu}(k) = \frac{-i}{k^2+i\varepsilon}\left[g_{\mu\nu}-(1-\xi)\frac{k_\mu k_\nu}{k^2}\right]} A_\nu + \sum_{i=1}^{2}-\phi_i^\dagger\underbrace{\left(\partial^2 + m_i^2\right)}_{\tilde{\Delta}_F(q^2)=\frac{i}{p^2-m^2+i\varepsilon}}\phi_i$$

$$+ \sum_{i=1}^{2}\underbrace{Q_i^2\,e^2\,\eta^{\mu\nu}}_{\times 2i \rightarrow 4-\text{vertex}} A_\mu A_\nu \phi_i^\dagger\phi_i \underbrace{- i\,e\,Q_i\,A_\mu\left(\phi_i^\dagger\partial^\mu\phi_i - \left(\partial^\mu\phi_i^\dagger\right)\phi_i\right)}_{\times i \rightarrow 3-\text{vertex}}.$$

Where in the last lines we identify the terms contributing to
the feyman rules. Our fields are given by the usual:

$$\phi(x) = \int\frac{d^3\mathbf{p}}{(2\pi)^{3/2}\sqrt{2\omega_\mathbf{p}}}\left[b_\mathbf{p}e^{-ip\cdot x} + c_\mathbf{p}^\dagger e^{ip\cdot x}\right]$$

$$\phi^*(x) = \int\frac{d^3\mathbf{p}}{(2\pi)^{3/2}\sqrt{2\omega_\mathbf{p}}}\left[b_\mathbf{p}^\dagger e^{ip\cdot x} + c_\mathbf{p}e^{-ip\cdot x}\right].$$

The Feynman rules are given in Table 5.2

Tbl 5.2: Feynman rules for SQED

for Every	write
internal photon line	$\tilde{D}_\xi^{\mu\nu}(\ell) =$ $\frac{-i}{\ell^2+i\varepsilon}\left[\eta_{\mu\nu} - (1-\xi)\frac{\ell_\mu\ell_\nu}{ell^2}\right]$
internal scalar	$\tilde{\Delta}_F(k^2) = \frac{i}{k^2-m^2+i\varepsilon}$

for Every	write
$\phi_i \phi_i^\dagger A_\mu A_\nu$ vertex	$2\mathring{i} Q_i^2 \, e^2 \, \eta^{\mu\nu}$
$\phi_i(k_i)\phi_i^\dagger(k_i') A_\mu$ vertex	$\mathring{i} e \, Q_i \, (k_i^\mu - k_i'^\mu)$
External scalar	$\times 1$
$\left\{ \begin{array}{c} \text{incoming} \\ \text{outgoing} \end{array} \right\}$ photon	$\times \left\{ \begin{array}{c} \varepsilon_\mu \\ \varepsilon_\mu^{*\prime} \end{array} \right\}$, with $\varepsilon \cdot k = 0, \varepsilon' \cdot k' = 0$

where we consider only incoming momenta and the arrows denote incoming or outgoing particles.

For the photon, we will take the Feynamn gauge, setting $\xi = 1$ and thus $\tilde{D}_1^{\mu\nu}(\ell) = \tilde{D}^{\mu\nu}(\ell) = \frac{-\mathring{i}\eta^{\mu\nu}}{\ell^2 + \mathring{i}\varepsilon}$. Notice that if we rescale all photon momenta (taking them to be the loop momenta) by $\hbar$ or equivalently take them to be in the soft region: $|k| \sim |q| \ll |p|$, where p is the external momenta, then the photon propagator scales homgenously in $\hbar$, typically:

$$\frac{1}{(\ell - q)^2} = \frac{1}{\hbar^2} \frac{1}{(\bar{\ell} - \bar{q})^2},\tag{5.20}$$

thus contributes $\mathcal{O}(\hbar^{-2})$ to the overall diagram. The matter propagator on the other hand, has inhomgenous $\hbar$ scaling, as we do not rescale the external momenta, (or equivalently the external momenta are not restricted by the regions). Note that we will not consider internal mass loops as the soft limit means that massive pair production is forbidden, thus massive propagators necessarily contain an external momentum. We can notheless expand a generic massive propagator in the soft limit:

$$\frac{1}{(\ell - p_i)^2 - m_i^2} = \frac{1}{\ell^2 - 2\ell \cdot p_i + \cancel{p_i^2} - \cancel{m_i^2}} = \frac{1}{\hbar^2\bar{\ell}^2 - 2\hbar\bar{\ell}\cdot p_i}$$

$$= -\frac{1}{\hbar}\frac{1}{2\bar{\ell}\cdot p_i}\left(1 + \hbar\frac{\bar{\ell}^2}{2\bar{\ell}\cdot p_i} + \hbar^2\frac{\bar{\ell}^4}{(2\bar{\ell}\cdot p_i)^2} + ...\right).\tag{5.21}$$

In other contexts one may say that the matter propagator has eikonalized (linearized). Before we compute the amplitudes let us set up some useful kinematic identities and variables. If we consider the two-to-two particle scattering, taking an all outgoing momentum convention we have the following masses:

$$m_1^2 = p_4^2 = p_1^2, \quad m_2^2 = p_2^2 = p_3^2, \qquad (5.22)$$

and mandelstam variables:

$$s = (p_1 + p_2)^2, \quad t = q^2 = (p_1 + p_4)^2, \quad u = (p_1 + p_3)^2,$$

subject to the usual constraint:

$$s + t + u = 2(m_1^2 + m_2^2).$$

We can also change the external momentum variables to ones more amenable to the soft limit, namely:

$$p_1 = -(\tilde{p}_1 - \frac{q}{2}), p_2 = -(\tilde{p}_2 + \frac{q}{2}), p_3 = (\tilde{p}_2 - \frac{q}{2}), p_4 = (\tilde{p}_1 + \frac{q}{2}).$$
$$(5.23)$$

The new momentum variables $\tilde{p}_i$ are crucially orthogonal to momentum transfer q :[53]

[53] we use 5.22

$$\tilde{p}_i \cdot q = 0,$$

and the physical scattering region, given by $s > (m_1 + m_2)^2$ and $q^2 < 0$ is the given by the same formulas:

$$s = \left(-(\tilde{p}_1 - \frac{q}{2}) - (\tilde{p}_2 + \frac{q}{2}) \right)^2 = (\tilde{p}_1 + \tilde{p}_2)^2$$
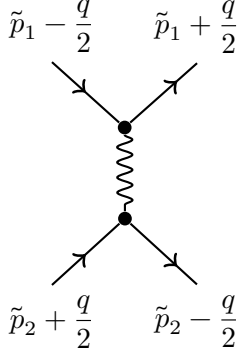
and

$$t = \left(-(\tilde{p}_1 - \frac{q}{2}) + \tilde{p}_1 + \frac{q}{2} \right)^2 = q^2.$$

With all the ingredients in place, we can now go on to computing the amplitudes.

5.5.1 Tree level

We start with the tree level amplitude, the only LO contribution in for example 5.18. The only possible diagram we can build with four external scalar legs, and vertices as defined in Table 5.2, is the following tree:

$$i\mathcal{A}^{(0)}(\tilde{p}_1 - \frac{q}{2}, \tilde{p}_2 + \frac{q}{2} \to \tilde{p}_1 + \frac{q}{2}, \tilde{p}_2 - \frac{q}{2}) \;=$$

Tree

The amplitude is read off diagram and using Feynman rules for SQED we have:

$$\mathcal{A}^{(0)} = i\mathring{\tilde{D}}^{\mu\nu}(q) \cdot e^2 Q_1 Q_2 2\tilde{p}_1{}^\mu 2\tilde{p}_2{}^\nu = \frac{4e^2 Q_1 Q_2 \tilde{p}_1 \cdot \tilde{p}_2}{q^2},$$

using the mandelstahm invariants described above we can infact write this as:

$$\mathcal{A}^{(0)} = e^2 Q_1 Q_2 \frac{4 m_1 m_2 \sigma}{\hbar^2 \bar{q}^2},$$

where σ is the relativistic factor of particle 1 in the rest frame of particle 2:

$$\sigma = \frac{s - m_1^2 - m_2^2}{2 m_1 m_2} = \frac{p_1 \cdot p_2}{m_1 m_2} = \frac{\tilde{p}_1 \cdot \tilde{p}_2}{m_1 m_2} + \mathcal{O}(\hbar). \qquad (5.24)$$

We now input the reduced version $\bar{\mathcal{A}}^{(0)} e^2 = \mathcal{A}^{(0)}$ of the amplitude, and take the $\hbar \to 0$ limit of 5.18. We can safely take the $\hbar \to 0$ limit as the integrand contains no terms singular in

$\hbar$ (the $\frac{1}{\hbar^2}$ is cancelled by the $\hbar^2$ pre-factor). Notice that the integration measure 5.12 simplifies in the classical limit:[54]

$$\lim_{\hbar \to 0} \mathrm{d}\overline{\Psi}(\bar{q}) = \tilde{\mathrm{d}}^4 \bar{q}\, \tilde{\delta}(2\widetilde{p_1 \cdot q})\tilde{\delta}(2\widetilde{p_1 \cdot q}).$$

The integrand corresponding to the LO contribution to the impulse is then:

$$\Delta p_1^{\mu,(0)} = 4e^2 Q_1 Q_2 m_1 m_2 \sigma \int \tilde{\mathrm{d}}^4 \bar{q}\, \mathrm{e}^{-i\bar{q}\cdot b} \bar{q}^\mu \frac{\cancel{\hbar^2}}{\cancel{\hbar^2}\bar{q}^2}.$$

This can be analytically computed (see LO impulse SQED) to find a closed form for the LO impulse.

$$\Delta p_1^{\mu,(0)} = -\frac{e^2 Q_1 Q_2}{2\pi} \frac{\gamma}{\sqrt{\gamma^2 - 1}} \frac{b^\mu}{b^2}$$

5.5.2 One loop

Already at one loop the number of possible diagrams one can for increases dramatically from 1 to 13. One can nonetheless relatively easily enumerate them. As we increase loop count, the number of diagrams increases exponentially. It is therefore very useful to have a systematic, programmatic way to handle these diagrams, and while we are at it, also to compute the amplitudes. Note that all the code needed to do these computations can be found on the repository for this book.

The first tool we will use is `QGRAF` **Nogueira:1993a**, a fortran program that can generate Feynman diagrams for a given set of vertices and external legs. The first step to is to define the theory we are working in. This is essentially writing down the Feyman rules, without actually specifying what the graphical objects are. For SQED the model file is short:

SQEDmodel

```
* propagators
[Phi1,Phi1c,+]
[Phi2,Phi2c,+]
[Photon,Photon,+]
```

[54] Compare to

$$\mathrm{d}\overline{\Psi}(\bar{q}) = \tilde{\mathrm{d}}^4 \bar{q}\, \tilde{\delta}(2p_1 \cdot \bar{q} + \hbar \bar{q}^2)\Theta(p_1^{\ 0} + q^0)$$
$$\tilde{\delta}(2p_1 \cdot \bar{q} + \hbar \bar{q}^2)\Theta(p_2^{\ 0} + q^0)$$

The theta functions cancel as $q^0 \to 0$ and p_i becomes classical. Changing to the special kinematic variables 5.23 we can even eliminate the delta functions, since by constuction $\tilde{p}_1 \cdot \bar{q} = 0$.

```
* vertices
  [Phi1c,Photon,Phi1]
  [Phi2c,Photon,Phi2]
  [Phi1c,Photon,Photon,Phi1]
  [Phi2c,Photon,Photon,Phi2]
```

This file also defines the names of the fields in question. We can then give `QGRAF` additional options, such as the number of external legs, and the number of loops, written in a `qgraf.dat` file that can look like this:

qgraf.dat

```
output= '{{output filename}}' ;
style= './styles/julia.sty' ;

model= './qgraf/SQEDmodel';

in= Phi1,  Phi2;
out= Phi1,Phi2;
loops= 1;
loop_momentum= k;

options=  notadpole,nosnail,onshell ;
```

where we specify what process we are interested in (two-to-two scattering). We also specify that we want to compute the one loop amplitude, and that we want to use the `julia.sty` style file. The `julia.sty` file is a style file that is used to generate the output in a format that can be read by a `Julia` [**Bezanson:2015**] package built to process and visualise the outputted graphs. This package is called (maybe too broadly) `QFT.jl` is hosted on github . Let us see it in action. We can run `QGRAF` from the command line, and it will generate a file called `{{output filename}}` that contains the output of the program. We can then use this in a `Julia` file to visualise the diagrams.

```
using Images
using QFT
using QFT.Diagrams
using QFT.FieldGraphs
```

```
using QFT.Fields
import  Catlab.Graphics.Graphviz: run_graphviz
include("SQED.jl")
diags=include("QGRAFout/julia/1lSQED.jl")


qDiags=[qDiagram(;diag...) for diag in diags]
grafs=(x -> x.g).(qDiags)

for (i,graf) in enumerate(grafs)
    open("./png/diag$i.png";create=true,write=true) do io
    run_graphviz(io,to_graphviz(graf),format="png")
    end
    display(Images.load("./png/diag$i.png"))
end
nothing
```

We can notice a few things about the diagrams above. Not all the diagrams contribute to the classical limit. Clearly the diagrams with internal matter loops cannot be allowed when the momenta incoming to the loop is soft [55]. In the classical limit this momenta will go to 0, and since the scalars are massive, they need momentum greater than their mass to be pair produced, thus these diagrams do not contribute. Another class of diagrams that does not contribute to the classical limit are the ones with photon loops that start and end on the same matter line. These do not contribute because they are scaleless. An integral is scaleless when its integrand $\mathcal{I}_{\text{scaleless}}(\{\ell_i\})$ scales homegenously under any rescaling of the loop momentum ℓ_i:

$$\mathcal{I}_{\text{scaleless}}(\{\ell_i\}) \xrightarrow{\ell_j \to \lambda \ell_j} \lambda^\eta \mathcal{I}_{\text{scaleless}}(\{\ell_i\})$$

Thus any diagram that has a basis of loops that does not contain both scalar fields (i.e. does not cross over) cannot have its scale set by the momentum transfer, and is thus scaleless. Dimensionally regularised scaleless integrals vanish, thus we can also discard these diagrams. We can easily implement such a filter programatically, by checking that if cycles are present they touch either both types of scalars, or neither. To compute the cycle basis we use an algorithm derived from

[55] scales like $\hbar$
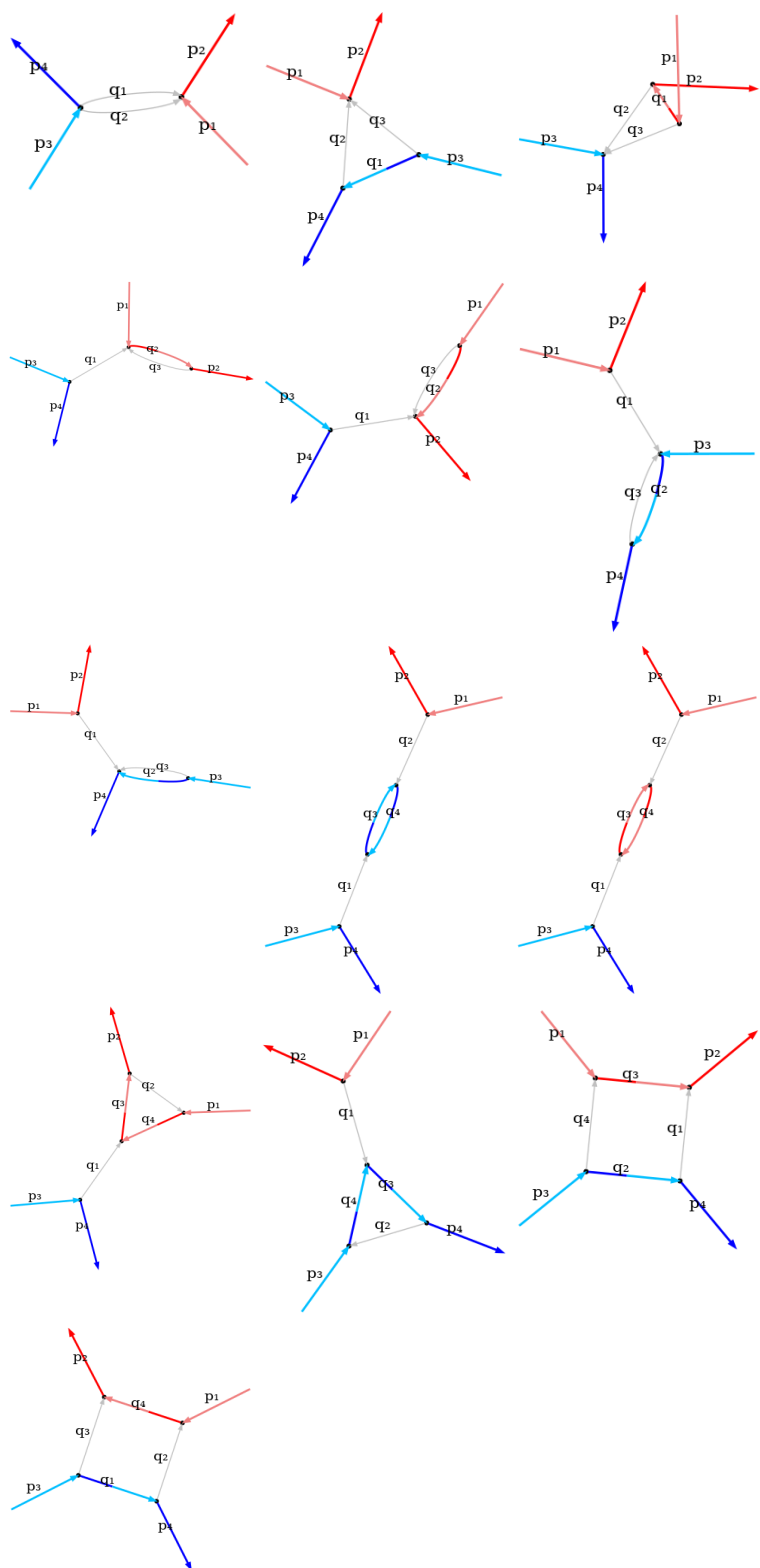
Paton:1969, implemented in the DirectedHalfEdgeGraphs.jl
package.

```julia
using Logging
Logging.disable_logging(Logging.Info)
function scaleless(g::AbstractFieldGraph)
  cycles =cycle_basis(g)
  isscaleless=false
  for c in cycles
    hs= collect(Iterators.flatten(half_edges.(Ref(g),c)))
    fields=unique!(typeof.(field.(Ref(g),hs)))
    if Bool(Phi1 in fields)   Bool(Phi2 in fields)
      isscaleless=true
    end
  end
  return isscaleless
end

noscalelessdiags=qDiags[.!scaleless.(grafs)]
classicaldiags=noscalelessdiags[2:end]
for (i,d) in enumerate(classicaldiags)
  d.ID=i
end
for (i,graf) in enumerate(grafs[.!scaleless.(grafs)])
    open("./png/diagscaleless$i.png";create=true,write=true) do io
    run_graphviz(io,to_graphviz(graf),format="png")
    end
    display(Images.load("./png/diagscaleless$i.png"))
end
nothing
```
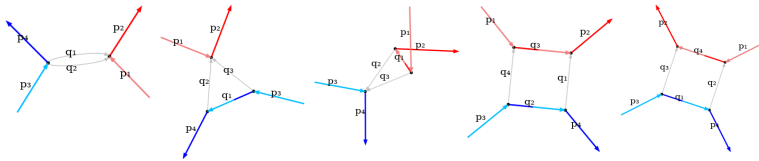

There is one final simplification we can do. The first diagram
above has two photon propagators, and two quartic vertices,
which give it its name: the double-seagull. The photon prop-
agators have homogeonous $\hbar^{-2}$ scaling (see 5.20), the vertices
only bring constants, and the loop integration has $\hbar^4$ scaling.
Together this means that the reduced amplitude has $\hbar^0$ scal-
ing. However in the virtual integrand the reduced amplitude

has to cancel with the transfer momentum's $\hbar$ scale (see 5.14). Thus the double seagull diagram dies in the classical limit.

We are left with only 4 diagrams, the two triangle diagrams, the box and cross box, which we can now compute. At this point we can do this manually, but again, putting in place a programattic framework means that subsequent loops can be treated systematically[56]. We will also extract one of these integrands by hand, for completeness and comparison.

The first step is to define the Feynman rules in a computer readable format. We will use `Julia` to apply these rules at every vertex and every edge, but for the actual computation we will use `FORM` [**Vermaseren:2000nd**, **Kuipers:2012rf**] which can automatically contract indices and does expression manipulations in an extremely fast way. The Feynman rules implementation in the package developped for this thesis make use of `Julias` defining paradigm of multiple dispatch. This allows us to define the rules for each vertex and each edge in a very compact way. We can define the rules as follows:

```julia
function feynmanRule(mime::MIME"text/FORM",p,f1::Photon,f2::Photon)
  momen = repr(mime,p.symbol)
  indx1 = repr(mime,index(f1))
  indx2 = repr(mime,index(f2))
  "_i* prop(-1,0,$momen)*d_($indx1,$indx2)"
end

@symmetric function feynmanRule(mime::MIME"text/FORM",p,[f1::Phi1,f2::Phi1c])
  momen = repr(mime,p.symbol)
  "_i* prop(-1,1,$momen)"
end

@symmetric function feynmanRule(mime::MIME"text/FORM",p,[f1::Phi2,f2::Phi2c])
  momen = repr(mime,p.symbol)

  "_i* prop(-1,2,$momen)"
end

@symmetric function feynmanRule(mime::MIME"text/FORM",[(p ,a)::Tuple{Any,ScalarField{S}},
          (p ,b)::Tuple{Any,AdjointField{ScalarField{S}}},(p , )::Tuple{Any,Photon}]) wh
  p1 = repr(mime,p (index( )))
  p2 = repr(mime,p (index( )))
```

```
    q = repr(mime,charge(a))
    "_i*e*$q*($p2-$p1)"
  end

  @symmetric function feynmanRule(mime::MIME"text/FORM",[(p , )::Tuple{Any,Photon},(p , )::
        (p ,b)::Tuple{Any,AdjointField{ScalarField{S}}},(p ,a)::Tuple{Any,ScalarField{S}}])
    mu = repr(mime,index( ))
    nu = repr(mime,index( ))
    q = repr(mime,charge(a))
    "2*_i*$q^2*e^2*d_($mu,$nu)"
  end
```

where we define `prop(n,i,p)` as representing a generic Feyn-
man propagator, which we will denote:

$$D_-(n,i,p) = \texttt{prop(n,i,p)} = (p^2 - m_i^2 + i\epsilon)^n \quad \text{thus} \quad \texttt{prop(-1,i,p)} = \frac{1}{p^2 - m_i^2 + i\epsilon}.$$

We can now apply these feynamn rules to the graphs we have
left, obtaining `FORM` readable integrands. For example the box
diagram gives:

```
  toform(stdout,classicaldiags[3])
```

```
*--#[d3l1:

L [d3l1|o.3.4|i.3.4|i|o|] = 1*i_* prop(-1,0,q1)*d_(nu1,nu2)*i_* prop(-
1,1,q2)*i_* prop(-1,2,q3)*i_* prop(-1,0,q4)*d_(nu7,nu8)*i_*e*qch1*(q2(nu1)-
p4(nu1))*i_*e*qch2*(q3(nu2)-p2(nu2))*i_*e*qch1*(p3(nu7)-
q2(nu7))*i_*e*qch2*(p1(nu8)-q3(nu8));
#procedure momentumRouting

Id q2 = p3 + -q4;
Id p1 = p2 + p4 + -p3;
Id q1 = p3 + -p4 + -q4;
Id q3 = p2 + p4 + q4 + -p3;

Id q4= l1;
#endprocedure
*--#]d3l1:
```

Notice that we also define the momentum routing by imposing the replacement rules, one per vertex. This can be done in many ways but to ensure proper scaling we set the loop momenta on the massless lines. This is done by the `Julia` program, using kruskal's algorithm [**Kruskal:1956**] to find the maximal-mass spanning tree of the graph, and then setting the loop momenta to be those internal edges that are missing from the tree. Using `FORM` we can contract indices and apply the momentum conservation rules. Finallly we also apply the relableing rules described in 5.23. The `FORM` version of the box integrand is then:

```
[d3l1|o.3.4|i.3.4|i|o|] =
      ( prop(-1,0,q - l1) )
    * ( prop(-1,0,l1) )
    * ( prop(-1,1,1/2*q - l1 + pb2) )
    * ( prop(-1,2, - 1/2*q + l1 + pb1) )
    * ( dot(l1,l1) )
    * ( dot(q,q) - 2*dot(q,l1) + dot(l1,l1) )
    * ( qch2 ) * ( qch2 ) * ( qch1 ) * ( qch1 )
    * ( e ) * ( e ) * ( e ) * ( e );
```

When applied to all 4 diagrams we obtain precisely the same integrands as those in **Kosower:2018adc**. Additionally we notice that the two triangles and the box diagram have overlapping propagators. In fact the denominators of the integrands for all three can be written as:

$$G_{i_1,i_2,i_3,i_4} = \frac{1}{\rho_1^{i_1} \rho_2^{i_2} \rho_3^{i_3} \rho_4^{i_4}}, \qquad (5.25)$$

for powers $\{i\} \in \{0,1\}^4$, where the inverse propagators ρ_i are:

$$\rho_1 = \ell^2 + i\epsilon, \quad \rho_2 = (\ell - q)^2 + i\epsilon, \quad \rho_3 = (-\frac{1}{2}q + \ell + \tilde{p}_1)^2 - m_1^2 + i\epsilon, \quad \rho_4 = (\frac{1}{2}q - \ell + \tilde{p}_2)^2 - m_2^2 + i\epsilon$$

Note that in the classical limit we can expand the massive propagators as shown in 5.21 and obtain to first order in $\hbar$:

$$\rho_3 = (-\frac{1}{2}q + \ell)^2 + 2\ell \cdot \tilde{p}_1 + i\epsilon, \quad \rho_4 = (\frac{1}{2}q - \ell)^2 - 2\ell \cdot \tilde{p}_2 + i\epsilon$$

The cross box can in fact extend this family, by adding just one more inverse propagator. We now have the complete description of the denominators of all 1-loop contributing diagrams. The numerators in fact do not complicate things much. They are all composed of scalar products of momenta. If these do not contain loop-momenta they are just constant factors in front of the integral. The scalar products that do contain loop momenta can be intelligently written as inverse powers of the propagators. This is the case for any feynman like integrand. Consider the following general integrand:

$$\mathcal{I} = \frac{\mathcal{N}}{\mathcal{D}} = \frac{\prod_{S'} N_{S'}}{\prod_{S} D_{S}} = \frac{\prod_{S'} \sum_{i \geq j} S'_{ij} p_i \cdot p_j}{\prod_{S} \sum_{i \geq j} S_{ij} p_i \cdot p_j},$$

where S and S' are sets of coefficient matrices for all possible dot products. If we have a quadruplet $\{A, B, a, b\}$ such that $A_{a,b} \neq 0$ and $B_{a,b} neq 0$ and p_a or p_b is a loop momentum ℓ, say $p_a = \ell$ then it is useful to write this component of the integrand as:

$$\frac{N_B}{D_A} = \frac{\tilde{N}_B + B_{ab} \ell \cdot p_b}{A_{ab} \ell \cdot p_b + \sum_{\substack{i \geq j \\ i,j \neq a,b}} A_{ij} p_i \cdot p_j} = \frac{\tilde{N}_B}{D_A} + \frac{B_{ab}}{A_{ab}} \left(1 - \frac{\tilde{D}_A}{D_A} \right).$$

where the tilde means that we have remove the *ab* contribution. Thus we see that we obtain in the numerator, a sum of objects, none of which contain the dot product: $\ell \cdot p_b$. We can do this for every quadruplet $\{A, B, a, b\}$, after every replacement and obtain an integrand containing only so called *irreducible* loop-momenta scalar products. In the cases we have here, they all dissapear, leaving us truely with a family of integrands like 5.25. This can be readily fed into a IBP solver, such as `AIR` [**Anastasiou:2004**], `FIRE` [**Smirnov:2020**] or `Kira` [**Maierhofer:2018**].

With such a solver we can obtain a complete family of integrals, that one can then look up. We are thus able to obtain the integrated integrands at NLO that are then used in 5.14 and 5.13.

We have now completed the program of NLO amplitudes

Add a section on everything together plus box and cross box
cancelation ()

6 Conclusion

In this thesis we explored the landscape of theoretical research that surrounds gravitational waves. We showed the existence of gravitational waves theoretically. We motivated waveform generation techniques grounded in first principles' physics. It is only through such precise frameworks that we can hope to elucidate the nature of the objects that emit this gravitational radiation. We looked at NR and EOB two complementary approaches to waveform generation that enabled LIGO to make that field changing detection in 2016. Both approaches have their challenges, NR with stability and computational cost, and EOB with higher order perturbative calculations. Each increase in precision enables a more precise match of the signal, enabling a much richer analysis of the incoming wave. Purely analytical tools have recently come into the crosshairs of particle physicits aswell.

We then went on to understand these nascent formalisms built on techniques from particle physics. The EFT matching approach enables a simple map from EOB to amplitudes computed in the potential kinematic region. This, and EOB in general, struggle to use and implement dissipation however. The Hamiltonian framework has to be somehow augmented with the dissipative forces. This motivates frameworks that sidestep the EOB framework. We explored the most developed one currently: KMOC. We were able to express classical observables such as the impulse in terms of the classical limit amplitudes and their unitarity cuts. We then went on to implement a programmatic framework for expressing the necessary integrals that the amplitudes yield. We used custom code to apply Feynman rules, manipulate and filter the graphs. We matched the results from **Kosower:2018adc**, and then implemented a scalar product reduction for preparing the input to IBP reduction programs.

The results and formalsims explored here show that amplitude techniques in gravitaional wave theory are a very promising

and powerful tool. A lot of the recent high energy physics results can directly be put to use in this context, and can already outperfom traditional methods. The higher perturbative order frontier however is increasingly difficult. At some point in the near future, these computations will have exhausted the techniques currently in use for particle physics. The next step is to develop new techniques that can be applied to both fields. Important work needs to be done to have a fully amplitude based waveform generation framework. This might be the next revolution in gravitational wave theory.

References